Equilibrium properties of granite pegmatite magmas

C. Wayne Burnham, Hanna Nekvasil*

Department of Geosciences, Pennsylvania State University, University Park, Pennsylvania 16802

While working toward that happy day when the formation of pegmatite minerals is much more thoroughly understood in terms of P-T-X conditions, it also should be of value to relate more satisfactorily the textural and structural features of the mineral aggregates to pegmatite-forming processes.

R. H. Jahns, in Jahns and Burnham (1969)

Abstract

Revision of the quasi-crystalline model has proceeded through a refinement of the cryoscopic equations for the major felsic melt components $NaAlSi_3O_8$ (*ab*), $CaAl_2Si_2O_8$ (*an*), $KAlSi_3O_8$ (*or*), and Si_4O_8 (*qz*), which has permitted more definitive identification and evaluation of the major speciation reactions that occur in the anhydrous and H_2O-saturated melts of the unary and binary subsystems of the system Ab-An-Or-Qz-H_2O. Application of this revised thermodynamic model to the investigation of melt speciation behavior in the system Ab-Or-Qz-Sil(sillimanite)-H_2O indicates the occurrence of a *sil*- and *qz*-consuming reaction to produce $Al_{1.455}Si_{2.91}O_8$ (*dpy* = dehydroxylated pyrophyllite). Similarly, application of the model to the system Ab-Qz-Eu(eucryptite)-H_2O at 2.0 kbar indicates the occurrence of a *eu*- and *qz*-consuming reaction, which forms a petalite-like species (*pe*) and greatly influences the positions of the liquidus field boundaries. Also, theoretical investigations of the shift in the haplogranite liquidus minimum upon addition of the volatiles F and B have led to the conclusion that these volatiles complex mainly with Na in the melt to form a cryolite-like and a sodium tetraborate–like melt species, respectively.

The effects of the proposed speciation reactions on the activities of the melt components in the expanded system Ab-An-Or-Qz-Co(corundum)-Sp(spodumene)-H_2O-F-B have been incorporated into the calculation of crystallization paths of the Spruce Pine, North Carolina, and Harding, New Mexico, pegmatites at 2.0 and 5.0 kbar. The resulting calculated sequences of crystallization show a strong correspondence with the change in major mineralogy of the inward succession of zones in these pegmatites, indicating magmatic control of the major mineralogy within each zone.

The compositions of chloride-free aqueous fluids reacted with Spruce Pine and Harding pegmatites and their melts up to 10 kbar indicate that the alkalis complex in these fluids with Al and Si in large polynuclear species similar to those in the coexisting melts. The addition of Cl, however, drastically depresses the aluminosilicate solubility and enhances that of the alkalis. The formation of perthite hoods and albitic lower zones in pegmatites can be attributed to the efficacy of transport of alkalis by a Cl-bearing aqueous phase in which the proportions of transported alkalis are determined by the equilibrium assemblage of each zone.

Introduction

Although "that happy day" may not yet have arrived, considerable progress has been made since 1969 in our understanding of the *P-T-X* conditions of pegmatite formation. This progress is a natural consequence of a growing body of knowledge regarding the provenance of granitoid rocks in general, the processes by which granitic magmas are generated, and especially the equilibrium properties of these magmas. From the results of the very

first experiments that Dick Jahns and one of us (C.W.B.) conducted on natural pegmatite material (Jahns and Burnham, 1957), it became apparent to both of us that a knowledge of the equilibrium properties of hydrous granitic magmas was prerequisite to a full understanding of pegmatite genesis. The quest for this knowledge, which has largely determined the course of a scientific career for almost 30 years, culminated in the development of a thermodynamic model (Burnham, 1981) that not only provides insight into the *P-T-X* conditions of pegmatite mineral formation, but also provides a rational basis for the interpretation of the heretofore unpublished (except as raw data in Clark, 1966) experimental results "that Dick

* Present address: Department of Chemistry, Arizona State University, Tempe, Arizona 85287.

kept talking about" (G. E. Brown, 1984, pers. comm.). In large measure, then, the model presented by Burnham (1981) and brought up to date in the next section is a tribute to the man we memorialize here, for it would not have been developed had Dick Jahns not persuaded one of us to undertake a comprehensive program of experimental research on hydrous silicate melts.

The model treats igneous rock melts as multicomponent solutions of chemically discrete and thermodynamically distinct neutral complexes or species that are correlated with thermodynamic components. Many of these species mimic the solid phases that crystallize from the melts in stoichiometry and presumably in the structure of their polyhedral elements. Those species that do not mimic the crystalline phases are linked to those that do through homogeneous speciation equilibria of two types: (1) simple dissociation, as in the incongruent melting products of the feldspars, and (2) interaction between two or more reactive species (components) to produce new species with different stoichiometries, hence different thermodynamic properties, as in the equilibrium reaction $KAlSi_3O_8$ (or) + 0.249 Si_4O_8 (qz) $\rightleftharpoons$ 0.687 $Al_{1.455}Si_{2.91}O_8$ (dpy) + 0.562 $K_{1.78}Si_{3.56}O_8$ (kts) (see next section; notation explained in App. 1).

The basis for this speciation model was the discovery that the activities (a_a^{am}) of the aluminosilicate components (feldspar-like species) in most anhydrous silicate melts, calculated from the basic cryoscopic equations through the expression

$$a_i^{am} = a_i^s \exp\left[-\left(\Delta G_{mi}^\circ + \int_{1\,bar}^{P} \Delta V_{mi}\, dP\right)/RT\right] \quad (1)$$

are either equal to or *less than* their corresponding mole fraction (X_a^{am}), when all nonvolatile components are chosen on the basis of equal numbers of oxygen atoms (eight) per formula unit and, therefore, of nearly equal molal volumes. This observation, when coupled with the assumption of ideal mixing of the aluminosilicate melt components [based on the theoretical implications of equimolal isothermal, isobaric H_2O solubilities in these melts (Burnham, 1975a; Burnham et al., 1978; Lasaga and Burnham, 1979)], led to the interpretation of the inequality of a_a^{am} and X_a^{am} as indicative of speciation.

The interpretation embodies the nontraditional[1] approach presented by the quasi-crystalline model. For pure components (i) and ideal component mixtures, the calculated melt activities are viewed as "true" mole fractions,

representing the actual amount of component i in the melt at a given P, T, and X_i^m. [Note that the assumption of ideal mixing of melt components, and hence of adherence to Raoult's law, requires that $a_i^{am} = X_i^{am}$ (true), but does not require that $a_i^{am} = X_i^{am}$ (experimental).] For melts in which $a_i^{am} \le X_i^{am}$, the difference between the experimental mole fraction and the activity of i, $X_i^{am} - a_i^{am}$, thus becomes a direct measure of the extent of speciation, on the assumption that the product species mix ideally with each other and with the reactant species (again on the basis of eight gram-atoms of oxygen per formula unit). Inasmuch as the extent of speciation is affected by pressure, volatile content (X_w^m), and composition, this difference is quantified by an equation of the form

$$X_i^{am} - a_i^{am} = X_i^{am} \cdot f(P, X_j^{am}, X_w^m), \quad (2)$$

where the superscript am refers to the anhydrous melt equivalent,[2] X_j^{am} represents the mole fractions of other nonvolatile components with which component i interacts chemically, and X_w^m is the mole fraction of H_2O in the melt. Alternatively, Equation 2 could have been written in terms of the stoichiometric activity coefficient ($\gamma_i^{am} \equiv a_i^{am}/X_i^{am}$), as $\gamma_i^{am} = 1 - f(P, X_j^{am}, X_w^m)$, but the correlation with the nature and extent of speciation would thereby have been obscured.

This quantification for the components ab, or, an, and qz was conducted through the use of published experimental liquidus data in systems of feldspar, feldspar-H_2O, feldspar-quartz, and feldspar-quartz-H_2O compositions from 1 bar to high pressure. The efforts of Burnham (1981) led to values of $X_i^{am} - a_i^{am}$ obtained from empirical fits to Equation 2, which, although varying systematically with the independent variables, were subject to difficultly assessable uncertainties from three sources: (1) experimental errors in the published P,T,X_i^{am} coordinates of crystal-melt equilibrium, (2) uncertainties in the standard-state Gibbs free energies of fusion (ΔG_{mi}° in Eq. 1), and (3) errors introduced at high pressures by the assumption that ΔV_{mi} in Equation 1 is independent of pressure and temperature throughout the P-T region of interest (Burnham, 1981, p. 205). This last source of error also compounded uncertainties in ΔG_{mi}° for sanidine (or, $KAlSi_3O_8$) and quartz (qz, Si_4O_8), because a constant ΔV_{mi} was employed for each of them, together with the albite-H_2O solution model (Burnham, 1981, p. 203–208), to derive internally consistent expressions for $\Delta G_{mor}^\circ/RT$ and $\Delta G_{mqz}^\circ/RT$. In an effort to minimize uncertainties from this source, the assumption of a constant ΔV_{mi} has been abandoned in favor of a pressure- and temperature-dependent ΔV_{mi}, as described in the next section. To further reduce uncertainties arising from the first and, to a lesser extent, second sources, new experimental data on the melting of feldspars and feldspar-quartz mixtures (Boettcher et al., 1982, 1984), as well as on the mixing properties of plagioclase feldspars at solidus temperatures (Carpenter, 1983, pers. comm.), have been used to revise the cryoscopic equations and the $X_i^{am} - a_i^{am}$ relations in the system $NaAlSi_3O_8$-$KAlSi_3O_8$-$CaAl_2Si_2O_8$-Si_4O_8-H_2O.

---

[1] From the more traditional standpoint, components for which $a_i^m \ne X_i^m$ (experimental) in a mixture of i and j could be viewed as exhibiting nonideal mixing behavior, giving rise to γ_i^m (P,T,X_j) ≤ 1.0 (for the components ab, an, or, and qz) and corresponding negative heats of mixing. For pure melts, a_i^m could be forced to 1.0, although this would result in unreasonable ΔV_{mi} (cf. Boettcher et al., 1982; Navrotsky et al., 1982). We believe that such an approach, however, does not hold as much promise of revealing the identity of melt units and mixing properties as that provided by the quasi-crystalline model.

[2] Mole fractions are normalized to an anhydrous basis to facilitate comparison with most published phase equilibria in hydrous systems, which also are presented on an anhydrous basis. Reconstitution involves application of Equations 3–6 and those in Tables 1 and 2.

The albite-H_2O solution model (Burnham and Davis, 1974; Burnham, 1975b) is an integral part of the development of expressions for $X_i^{am} - a_i^{am}$ in that it dictates the relationship among a_w^m, a_i^{am}, and a_i^{hm} through application of the Gibbs-Duhem relation to expressions for a_w^m. The a_w^m is given by the following relations (Burnham, 1975b):

$$a_w^{mi} = k_w^{mi}(X_w^{mi})^2 \quad \text{for } X_w^{mi} \leq 0.5 \tag{3}$$

and

$$(a_w^{mi}) = 0.25 k_w^{mi} \exp\left[\left(6.52 - \frac{2667}{T}\right)(X_w^{mi} - 0.5)\right]$$
$$\text{for } X_w^{mi} > 0.5 \tag{4}$$

where k_w^{mi} is the Henry's law analogue constant for the solution of H_2O in melt of composition i. For melts of feldspar composition, values of $\ln k_w^{ma}$ as a function of pressure and temperature are presented in Figure 1 (cf. Fig. 9.2 of Burnham, 1981) and for melts of Si_4O_8 composition, $\ln k_w^{mqz} = \ln k_w^{ma} + 0.47$ (Burnham, 1981, p. 206). In accordance with the interpretation placed on this difference (loc. cit.), which is consistent with the higher H_2O solubilities in peraluminous melts found by Dingwell et al. (1984), $\ln k_w^{mi} = \ln k_w^{ma} + 0.47(1 - N_{Al}^{mi})$, where N_{Al}^{mi} is the number of gram-atoms of Al per 8-oxygen formula weight of component i.

Hence, from the Gibbs-Duhem relation, the activity of i in hydrous melts obeys the relations (Burnham, 1981, p. 205)

$$a_i^{hm} = a_i^{am}(1 - X_w^m)^2 \quad \text{for } X_w^{mi} \leq 0.5 \tag{5}$$

and

$$a_i^{hm} = 0.25 a_i^{am} \exp\left[\left(6.52 - \frac{2667}{T}\right)[\ln(1 - X_w^m) + X_w^m + 0.193]\right]$$
$$\text{for } X_w^{mi} > 0.5. \tag{6}$$

Following a discussion of revisions in the cryoscopic and $X_i^{am} - a_i^{am}$ equation in the next section, the revised relations will be used in conjunction with experimental liquidus data in simple systems not only to illustrate the nature and principles of speciation in aluminosilicate melts, but also to clarify some misconceptions regarding the speciation model that have arisen in the literature. Next, the previously unpublished experimental results of Burnham and Jahns on the composition of aqueous fluids reacted with the Harding, New Mexico, and Spruce Pine, North Carolina, pegmatites and their melts, coupled with other published data on volatile-melt equilibria, will be interpreted within the framework of the speciation model. Then, the crystallization paths of the two pegmatite magmas will be calculated from the thermodynamic model and compared with experimentally determined melting relations. Finally, model calculations and experimental results on crystal–melt–aqueous fluid equilibria will be combined in an effort to gain new insights into the role of magmatic processes in pegmatite formation.

REVISED THERMODYNAMIC MODEL

Quantification of the extent of speciation of i in silicate melts, $X_i^{am} - a_i^{am}$, and identification of the primary speciation reaction, is dependent upon the calculated activities of i. Along any univariant melting curve of I (or I +
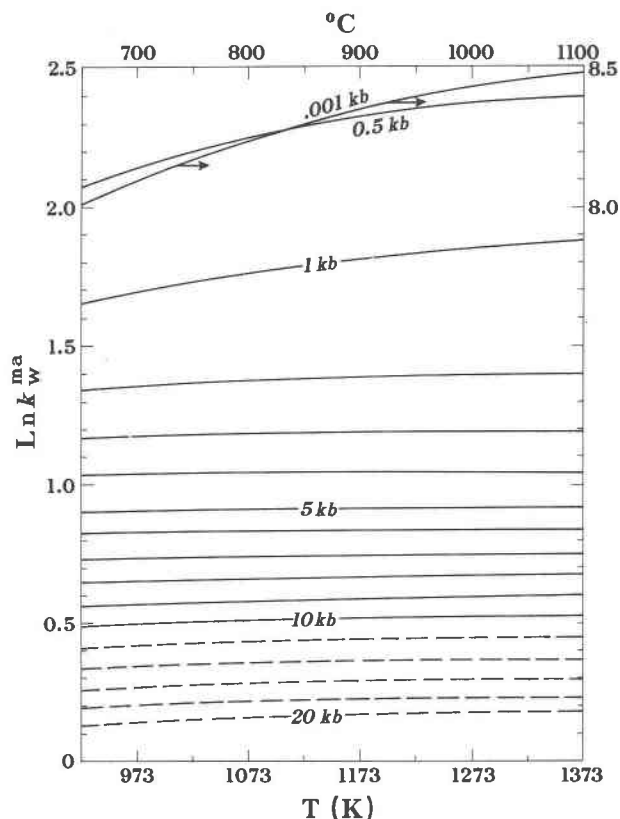

Fig. 1. The pressure and temperature dependence of the Henry's law analogue constant for H_2O in feldspar melts, from Burnham (1979a, 1979b, 1981). See text for applicability to other silicate melts.

J), the equality dictated by the basic equation of equilibrium must hold. For equilibrium between component i in crystal and melt, Equation 1 describes this equality. The calculation of a_i^{am} in the melt along a melting curve of i thus requires the evaluation of the cryoscopic equation for $i[(\Delta G_{mi}^\circ + \int_{1\,\text{bar}}^{P} \Delta V_{mi}\,dP)/RT]$ at each P and T. (As described by Burnham, 1981, the standard state here is a hypothetical one in many cases, as it refers to pure, undissociated i in the melt or crystalline state at P and T.) The calculation of liquidus relations, however, involves both an analytic expression for the cryoscopic equation and expressions for $X_i^{am} - a_i^{am}$ as $f(P,T,X_j^{am})$ (cf. Eq. 2). It also requires the use of a mixing model for components in solid solution (needed in the evaluation of a_i^s, which, in the Ab-Or-An-Qz-H_2O compositional volume are essentially restricted to those in plagioclase (Carpenter, 1983, pers. comm.; Blencoe et al., 1982) and alkali feldspar (Thompson and Hovis, 1979) solid solutions.

Cryoscopic equations

Analytic expressions were derived for $\Delta G_{mi}^\circ/RT$ as $f(T)$ in the form $\Delta G_{mi}^\circ/RT = a + b/T + c \ln T$, for the components ab, an, or, and qz (Si_4O_8). This formulation forces ΔH_{mi}° to vary linearly with temperature, which, in turn, results in a constant $\Delta C_{P,mi}$.

Table 1a.   Cryoscopic equations for albite, anorthite, sanidine, and quartz at 1 bar: $\Delta G^\circ_{mi}/RT = a + b/T + c \ln T$; $T \equiv$ temperature in kelvins

Component i	Coefficients a	b	c
ab (NaAlSi$_3$O$_8$)	10.59	4578	-1.918
an (CaAl$_2$Si$_2$O$_8$)	56.41	1743	-7.636
or (KAlSi$_3$O$_8$)	19.55	3835	-3.017
qz (Si$_4$O$_8$)	21.80	811.6	-2.983

Expressions for $\Delta G^\circ_{mab}/RT$ and $\Delta G^\circ_{man}/RT$ were derived simultaneously, for internal consistency, with the following requirements: (1) The relation between $\Delta G^\circ_{mab}/RT$ (for high albite) and $\Delta G^\circ_{man}/RT$ must be preserved through the expression $\Delta G^\circ_{man}/RT - \Delta G^\circ_{mab}/RT = \ln(a^s_{an}a^m_{ab}/a^m_{an}a^s_{ab})$. This necessitates (a) the use of approximations for γ^{Pl}_{an} and γ^{Pl}_{ab} at 1 bar (Carpenter, 1983, pers. comm.), (b) the assumption of Raoultian mixing between ab and an in the melt, (c) the assumption that, at 1 bar, there is no dissociation of either ab or an, and (d) the use of the 1-atm plagioclase melting loop of Bowen (1913). (2) The restrictions provided by available calorimetric data on ΔH°_{mi} and $\Delta G^\circ_{mi(298)}$ must be preserved.[3] (3) The additional restrictions provided by the 1-bar melting temperature of pure anorthite (1830 K, Robie et al., 1978) and albite[4] (1391 K, Schairer and Bowen, 1956) must also be maintained. The data of Robie and Waldbaum (1968) for albite and albite glass were used as a first-order approximation to initiate the iterative process.

Expressions for $\Delta G^\circ_{mor}/RT$ and $\Delta G^\circ_{mqz}/RT$ could not be obtained directly from calorimetric data, owing to the strong speciation of or at 1 bar (manifested by its strong incongruency at this pressure) and uncertainties associated with the crystalline polymorphs of SiO$_2$. These expressions were derived, instead, from phase-equilibrium data. For sanidine, as in Burnham (1981), the Or-H$_2$O system was used because of the congruent-melting behavior at pressures above 2.6 kbar (Goranson, 1938). Use of these data above 2.6 kbar (Lambert et al., 1969) required that (1) the albite-H$_2$O model (Eqs. 3–6) be used to convert activities from an anhydrous basis to their hydrous equivalents; (2) an assumption be made that the or component does not dissociate in the Or-H$_2$O system at pressures above approximately 5 kbar (i.e., $a^{am}_{or} = 1.0$ along the H$_2$O-saturated solidus); (3) the ΔH°_{mor} obtained from the resulting $\Delta G^\circ_{mor}/RT$ equation at the metastable melting temperature of pure sanidine (1513 K) be consistent with that calculated from Stebbins et al. (1983) and that the $\Delta G^\circ_{mor(298)}/RT$ fall within the range 11.9–17.4 of Robie et al. (1978); (4) expressions for ΔV_{mor} be used which were obtained from available data on V^{os}_{Or}, $\alpha^s_{Or}(T)$ and $\alpha^g_{Or}(T)$ and $\beta^s_{Or}(P)$. Where reliable data were not available (i.e., β^g_{Or}, V^{og}_{Or}), approximations were made using the data for quartz, albite, and anorthite.

The resulting expression for $\Delta G^\circ_{mor}/RT$ in Table 1 required that the metastable melting point of Waldbaum (1968) at 1473±40 K be moved to 1513 K, which, coincidentally, is the same temperature as that used by Hervig and Navrotsky (1984) in their calculation of the binary melting relations of Ab-Or from heats of mixing.

For quartz, the anhydrous melting curve of Jackson (1976) was combined with the lower-temperature data along the H$_2$O-saturated quartz solidus of Kennedy et al. (1962) and Stewart (1967).[5] The reduction of these data into an expression for $\Delta G^\circ_{mqz}/RT$ necessitated use of thermal expansion and compressibility data to obtain $\Delta V_{mqz}(P,T)$. No constraint was imposed on $\Delta G^\circ_{mqz(298)}/RT$ owing to the uncertainties associated with the α-β quartz transition.

The $\Delta G^\circ_{mi}/RT$ expressions are summarized in Table 1 and graphed in Figure 2. These expressions differ from those of Burnham (1981) owing to use of more recent calorimetric data as constraints imposed on $\Delta G^\circ_{mi}/RT$, use of approximated activity coefficients for the plagioclase solid solution, and use of thermal expansion and compressibility data to obtain $\Delta V_{mi}(P,T)$.

---

[3] Constraints imposed: $\Delta H^\circ_{man} = 32\pm2.1$ kcal (Weill et al., 1980) at T_{man}; $\Delta H^\circ_{mab} = 15.5\pm2$ kcal (Stebbins et al., 1980) at T_{mab}; $\Delta G^\circ_{man(298)}/RT = 21.8$–27.0 (Robie et al., 1978); $\Delta G^\circ_{mab(298)}/RT = 13.3$–18.6 (Robie and Waldbaum, 1968).

[4] The melting temperature of 1373 K determined by Boettcher et al. (1982) does not permit preservation of the above restrictions in that ΔH°_{mab} becomes too high, unless the entire cryoscopic curve obtained from the data of Robie and Waldbaum (1968) is lowered by 18 K.

[5] The data of Stewart (1967) differed at pressures above 2 kbar from those of Kennedy et al. (1962); hence, a melting curve was constructed that lay within the temperature range provided by these workers, with the restrictions that the modified solidus and ensuing $\Delta G^\circ_{mqz}/RT$ must describe smooth curves with temperature.

Table 1b.   Pressure dependence of cryoscopic equilibria:

$$\int^P_{1\ bar} \Delta V_{mi}\, dP/RT = [a(P - 1.0) + b(P^2 - 1.0) + c(P^3 - 1.0) + d(P^4 - 1.0)]/T;$$

$T \equiv$ temperature in kelvins, $P \equiv$ pressure in bars

Component i	Coefficients a	b	c	d
ab**	$0.1081 - 7.569\times10^{-6}T - 1.133\times10^{-8}T^2$	-0.7051×10^{-6}	0.9180×10^{-11}	0
an***	$0.1187 - 5.028\times10^{-6}T - 0.7526\times10^{-8}T^2$	-0.5981×10^{-6}	0.7780×10^{-11}	0
or†	$0.1055 - 1.029\times10^{-5}T$	-0.7360×10^{-6}	1.0980×10^{-11}	-2.319×10^{-17}
qz†† (Si$_4$O$_8$)	$0.1277 + 4.761\times10^{-5}T - 2.274\times10^{-8}T^2$	-0.7242×10^{-6}	0.9146×10^{-11}	0

Sources of data on thermal expansions, compressibilities, and standard-state molar volumes of crystals and glasses:

**Robie et al. (1978); Ghiorso et al. (1979); Arndt and Haberle (1973) (β^s_{Ab} and β^g_{Ab} are approximated).

***Robie et al. (1978); Ghiorso et al. (1983); Arndt and Haberle (1973) (α^s_{An}, β^g_{An} and V^{og}_{An} are approximated).

†Robie et al. (1978); Orlowski and Koenig (1941); Birch (1966); Arndt and Haberle (1973), (β^g_{Or} and V^o_{Or} are approximated).

††Robie et al. (1978); Ghiorso et al. (1979); Birch (1966); Skinner (1966).

Melt speciation

The derived cryoscopic equations (Table 1 and Fig. 2) permit the calculation of a_i^{am} in all bounding unary and binary subsystems of the anhydrous or hydrous system Ab-An-Or-Qz, provided that a crystalline phase containing component i is in equilibrium with the melt. Although these calculated activities of i at P, X_w^m, and X_i^{am} (and, hence, calculated values of $X_i^{am} - a_i^{am}$) indicate the extent of speciation, they do not necessarily contain unequivocal information regarding either the number of species formed or their nature. The number of species formed is limited by the fact that the mole fractions of all species (components) must sum to unity and by the Gibbs phase rule in the generalized form, $F = N - R - P + 2$, where N is the total number of species (components) and R is the number of restrictive conditions that can be placed on the equilibria involving the reactive components (Gibbs, 1961; Denbigh, 1971; Boettcher and Burnham, 1983). The nature of the species formed, on the other hand, is not always unambiguous, but insight often can be gained from (1) the appearance of a crystalline phase with the stoichiometry of a possible speciation product, (2) the $X_i^{am} - a_i^{am}$ behavior of one or more other components in the system, (3) the behavior of $X_i^{am} - a_i^{am}$ as a function of pressure and H_2O content of the melt, and (4) what is known or can be inferred regarding the relative stabilities of the various candidate compounds as functions of pressure, temperature, and bulk composition of the system.

In the anhydrous and H_2O-saturated unary systems, speciation reactions were proposed according to the crystalline phases appearing at singular or nondegenerate invariant points. Such proposed speciation reactions can be tested only in the special cases when another phase appears for which the activity of the corresponding melt component can be calculated independently through its cryoscopic equation (permitting comparison between the stoichiometrically obtained activity and the calculated activity). In the Qz-bearing binaries, however, the proposed speciation reactions can be readily tested by comparison of the eutectic compositions, calculated by combining the computed a_a^{am} and a_{qz}^{am} along the generalized A + Qz ⇌ L curve and the stoichiometric constraints provided by the speciation reactions themselves, with the eutectic compositions obtained experimentally.

Speciation by dissociation in albite ($NaAlSi_3O_8$) melts. The effect of pressure on the degree of dissociation of ab along the high-pressure melting curve of albite (Boettcher et al., 1982) was evaluated using the derived cryoscopic equation for albite in Table 1. Above 1 bar, the calculated a_{ab}^{am} is consistently lower than the experimental mole fraction ($X_{ab}^{am} = 1.0$). The extent of dissociation, $X_{ab}^{am} - a_{ab}^{am}$, increases strongly with increasing pressure, levels off at approximately 12 kbar, and begins to increase again as the invariant point Ab + Qz + Jd + L is approached at 33.3 kbar (Boettcher et al., 1982, 1984; Bell and Roseboom, 1969).

It is postulated that this change in the rate of increase in degree of speciation with pressure is suggestive of a change in the speciation reaction to one that involves
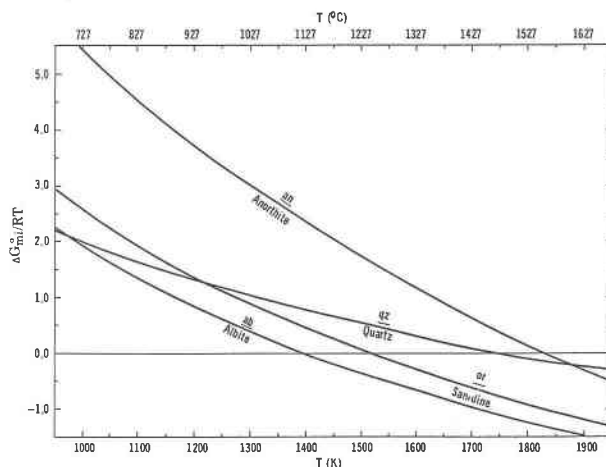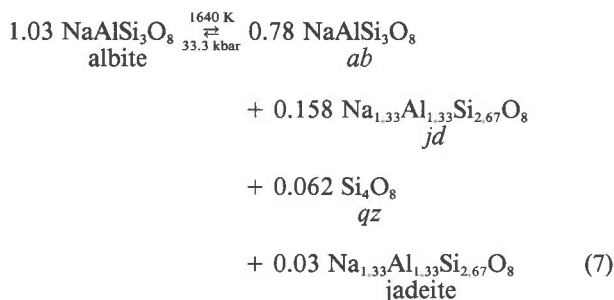

Fig. 2. The temperature dependence of the 1-atm cryoscopic equations for the feldspars and quartz, calculated from equations in Table 1.

formation of a jadeite-like melt species.[6] At the invariant point, for example, the proposed reaction can be directly tested by comparison of the a_{qz}^{am} obtained stoichiometrically, through $X_{ab}^{am} - a_{ab}^{am}$, with that obtained via the cryoscopic equation for quartz. The calculated activity of ab in the melt at 33.3 kbar and 1640 K is 0.78, whereas at 33.3 kbar and 1650 K, which is on the metastable extension of the univariant melting curve of albite (Boettcher et al., 1982), $a_{ab}^{am} = 0.82$. Hence, at the invariant point, 3 mol% jadeite ($Na_{1.33}Al_{1.33}Si_{2.67}O_8$) is in equilibrium with a melt that contains 1% excess Si_4O_8 (qz). Thus, if it is assumed that the new melt species formed consist only of jd and qz, which mix ideally with each other and with ab, then the melting reaction may be balanced stoichiometrically by

$$1.03\ NaAlSi_3O_8 \overset{1640\ K}{\underset{33.3\ kbar}{\rightleftarrows}} 0.78\ NaAlSi_3O_8$$
albite $\qquad\qquad\qquad ab$

$$+\ 0.158\ Na_{1.33}Al_{1.33}Si_{2.67}O_8$$
jd

$$+\ 0.062\ Si_4O_8$$
qz

$$+\ 0.03\ Na_{1.33}Al_{1.33}Si_{2.67}O_8 \qquad (7)$$
jadeite

where, at an equilibrium involving albite, jadeite, quartz, and melt, $X_{qz}^{am} = a_{qz}^{am} = 0.062$. The cryoscopic equation for

---

[6] In the authors' opinion, which is shared by at least one expert in spectral analysis (W. B. White, 1985, pers. comm.), structural interpretations based on spectral analyses of glasses are not sufficiently definitive at the present time to warrant an attempt here to reconcile differences in interpretation.

quartz (Table 1) yields $a_{qz}^{am} = 0.057$ at this pressure and temperature!

This remarkable agreement between the mole fraction of qz required to balance the speciation reaction of ab and the independently calculated activity of qz has several important ramifications. First and foremost, it is strong confirmatory evidence for the validity of the speciation model. Second, it supports the assumption in the derivation of the cryoscopic equations that the compressibility of the ab component in the melt is essentially the same as that of Si_4O_8 melt. Third, it demonstrates the internal consistency in the standard-state (T, 1 bar) cryoscopic equations for albite and quartz, which were derived from different sets of data. Fourth, it confirms the presence of a species that has the stoichiometry of jadeite; it does not, however, shed direct light on the structure (Al coordination) of this species.

That the structure of this species does, indeed, mimic that of jadeite is suggested by other experimental data and the $X_{ab}^{am} - a_{ab}^{am}$ relations. The experimental data of Kushiro (1980, Figs. 6 and 7) indicate that the viscosity of albite melts decreases, whereas the density increases markedly, at pressures between approximately 13 and 20 kbar. These relationships were interpreted by Kushiro to indicate an abrupt change to a less-polymerized, denser structure of the melt over this pressure interval, as would occur if part of the Al in the melt were to shift into sixfold coordination. Similarly, the curve for $X_{ab}^{am} - a_{ab}^{am}$ versus pressure appears to approach a maximum of 0.20 at 12–14 kbar, pass through an inflection and increase again slightly to 0.22 at 33.3 kbar. The large increase in $X_{ab}^{am} - a_{ab}^{am}$ up to 12 kbar, concomitant with a smooth decrease in viscosity (Kushiro, 1980, Fig. 6),[7] is consistent with the speciation reaction

$$NaAlSi_3O_8 \rightleftarrows 0.687\ Al_{1.455}Si_{2.91}O_8 + 0.313\ Na_{3.2}Si_{3.2}O_8, \quad (8)$$
$$\quad ab \qquad\qquad\qquad dpy \qquad\qquad\qquad nds$$
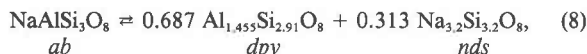
where nds is a sodium disilicate–like species which, like dpy, presumably has a sheet structure. As pressure is increased above 14 kbar, however, and dpy and nds react further to produce jd and qz, as in Reaction 7, very little additional ab is required to dissociate in order to maintain the ab-jd-qz equilibrium.
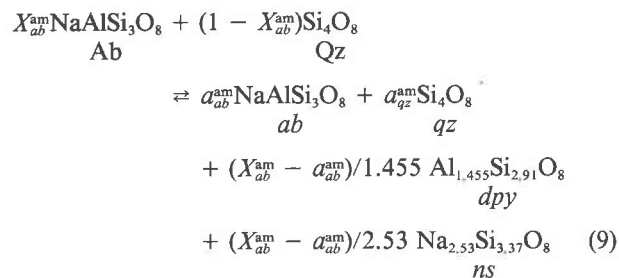
This reaction scheme requires that at least five melt species, which are equated with thermodynamic components, be in homogeneous equilibrium along the univariant melting curve of albite between approximately 15 and 20 kbar. For the equilibrium to be univariant ($F = N - R - P + 2 = 1$) in a system where $N = 5$ and $P = 2$, however, there must be four restrictions ($R = 4$) that can be placed on the equilibria among the five reactive components in Reactions 7 and 8. These four restrictions consist of two equilibrium constants and two fixed ratios of speciation reaction products; hence, the system is just as univariant as if albite melt had been treated as a one-component system (cf. Navrotsky et al., 1982; Boettcher and Burnham, 1983).

In order to determine the effect of X_w^m on a_{ab}^{am}, activities of ab were computed along the H_2O-saturated solidus of Bohlen et al. (1982), Erikson (1979), and Tuttle and Bow-

en (1958). The addition of H_2O to albite melt at high pressures appears to enhance the extent of dissociation. This effect of H_2O pressure, which cannot be separated from the effects of much lower equilibrium temperatures, may reflect the formation of an analcite-like melt species.

Speciation by interaction in the system $NaAlSi_3O_8$-Si_4O_8-H_2O. Luth (1969) determined the P-T relations of the anhydrous solidus in the system Ab-Qz from 8 to 20 kbar, as well as the shift in eutectic composition over this pressure range. As anticipated, owing to the intersection of the Ab + Qz solidus with the Ab + Jd solidus at the invariant point, Ab + Jd + Qz + L (33.3 kbar, Bell and Roseboom, 1969), the eutectic composition shifts markedly toward the Ab sideline with pressure (from ~67 wt% Ab at 8 kbar to ~88 wt% Ab at 20 kbar). Boettcher et al. (1984) redetermined the Ab + Qz solidus and obtained temperatures approximately 60°C lower than those of Luth (1969). They also determined a eutectic composition of 96 ± 1 wt% $NaAlSi_3O_8$ at 15 kbar, which is much more albitic than the 80 wt% composition obtained by extrapolation of Luth's 15-kbar data.[8] It is also inconsistent with a eutectic temperature that is 50°C lower than the melting point of pure albite (Boettcher et al., 1984, Fig. 2).

In view of these discrepancies and inconsistencies, it seemed inadvisable to attempt a derivation of the pressure dependence of $X_{ab}^{am} - a_{ab}^{am}$ using either eutectic composition. Instead, the more recently determined eutectic temperatures of Boettcher et al. (1984) were combined with an assumed speciation reaction

$$X_{ab}^{am}NaAlSi_3O_8 + (1 - X_{ab}^{am})Si_4O_8$$
$$\quad Ab \qquad\qquad\qquad Qz$$

$$\rightleftarrows a_{ab}^{am}NaAlSi_3O_8 + a_{qz}^{am}Si_4O_8$$
$$\qquad\quad ab \qquad\qquad\qquad qz$$

$$+ (X_{ab}^{am} - a_{ab}^{am})/1.455\ Al_{1.455}Si_{2.91}O_8$$
$$\qquad\qquad\qquad\qquad\qquad dpy$$

$$+ (X_{ab}^{am} - a_{ab}^{am})/2.53\ Na_{2.53}Si_{3.37}O_8 \quad (9)$$
$$\qquad\qquad\qquad\qquad\qquad ns$$

to calculate eutectic compositions using the relationships among the stoichiometric coefficients, which reduce to $X_{ab}^{am} = 0.923(1 - a_{qz}^{am}) + 0.077a_{ab}^{am}$, and the cryoscopic equations in Table 1 to obtain a_{ab}^{am} and a_{qz}^{am}. This speciation reaction, which yields a eutectic composition of $X_{ab}^{am}(E) = 0.85$ at 15 kbar, is similar to that proposed above for the lower-pressure dissociation in pure albite melts (Eq. 8), except the nds in that reaction is presumed here to combine with excess Si_4O_8 and form ns (cf. Burnham, 1981, p. 215). Without this presumption, $X_{qz}^{am} - a_{qz}^{am}$ would have been zero, and the calculated eutectic—assuming nds formation—would have shifted only approximately 1.0 mol% toward the albite sideline. Thus, the calculated eutectic

---

[7] Were it not for depolymerization accompanying $dpy + nds$ speciation, the viscosity should increase with increasing pressure (Scarfe, 1984).

[8] This composition was obtained by extrapolating the quartz liquidus, which was interpolated between that obtained by Luth (1969) at 20 kbar and at 10 kbar, to the solidus temperature of Boettcher et al. (1984) at 15 kbar.

composition is not very sensitive to the nature of the sodium silicate species present, owing to the small differences in stoichiometry of *ns* and *nds*; perhaps both *ns* and *nds* are present in these relatively *qz*-poor melts. The fact that the use of Reaction 9 yields a calculated eutectic composition that lies well within the range of experiment, however, justifies the assumption that the principal sodium silicate species in melts of the Ab-Qz system is *ns*. The $X_i^{am} - a_i^{am}$ relations in the system Ab-Qz-H₂O, as described below, lend strong support to this assumption.
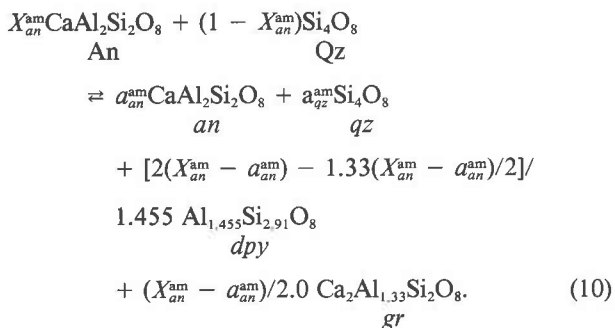
The system Ab-Qz-H₂O under H₂O-saturated conditions was investigated using the Ab + Qz (+ H₂O) ⇌ L (+ V) solidus of Tuttle and Bowen (1958) for pressures of 1 to 3 kbar, that of Luth et al. (1964) for 5 kbar, and that of Boettcher and Wyllie (1969) for 10 kbar. The a_{ab}^{hm} and a_{qz}^{hm} were converted to an anhydrous basis using Equations 5 and 6 once the saturated mole fraction of H₂O (X_w^msat.) was calculated at each pressure from Equations 3 and 4. These activities of the melt components, when inserted into Reaction 9, yield eutectic compositions which agree with the experimentally determined eutectic compositions within ±1.0%! This agreement indicates that Reaction 9, assumed to describe the speciation behavior in the anhydrous system Ab-Qz, is reasonable and that the addition of H₂O, although increasing the degree of dissociation, does not change the nature of the speciation reaction, except for hydroxylation.

Speciation by dissociation in anorthite ($CaAl_2Si_2O_8$) melts. The high-pressure curve of Boettcher et al. (1984) was used to determine the effect of pressure on the dissociation of *an*. This curve intersects the singular point An ⇌ Co + L (Co = corundum) at approximately 9.4 kbar. Beyond this singular point, the anorthite melting curve shows an increasingly negative slope. The variation of $X_{an}^{am} - a_{an}^{am}$ along this melting curve follows a smooth curve with pressure, increasing less rapidly as pressure is increased. Although this indicates that no major change in speciation reactions takes place with pressure, the identification of a unique reaction is problematic. The fact that the melting curve of anorthite first reaches a point of incongruency (Co + L) and then intersects the invariant point Cts + An + Co + Ky + L (Wood, 1978) or Cts + Qz + An + Co + L (Hariya and Kennedy, 1968) suggests that several, if not all, of these crystalline phases have counterparts in the melt. If this is the case, then several reactions may be taking place simultaneously.

The An-H₂O system was investigated along a melting curve obtained using data of Erikson (1979) and Yoder (1954) at higher pressures. The addition of H₂O, as for albite melt, initially depresses dissociation, but at pressures above 2 kbar enhances it considerably. Since the H₂O-saturated melting curve intersects the An ⇌ Co + L singular point at 9 kbar, and the invariant point An + Co + Zo + L + V (Zo = zoisite) above 14 kbar (Boettcher, 1970), it is reasonable to propose a reaction that involves the formation of *zo* (a dehydroxylated zoisite-like species) and *co*.

Speciation by interaction in the system $CaAl_2Si_2O_8$-Si_4O_8-H₂O. Investigation of the variation of $X_{an}^{am} - a_{an}^{am}$ with pressure in the anhydrous An-Qz binary system is complicated by the paucity of low-pressure data on the An + Qz ⇌ L univariant curve. Boettcher et al. (1984) determined the *P-T* relations of this solidus at 1 bar and

pressures above 12 kbar and obtained approximate eutectic compositions at 1 bar and 18 kbar. If these compositions are combined with an interpolated melting curve and the restriction that $X_{an}^{am} - a_{an}^{am}$ must remain greater than zero, it is possible to postulate the following general reaction:

$$X_{an}^{am}CaAl_2Si_2O_8 + (1 - X_{an}^{am})Si_4O_8$$
$$\quad\quad An \quad\quad\quad\quad\quad\quad\quad Qz$$

$$\rightleftharpoons a_{an}^{am}CaAl_2Si_2O_8 + a_{qz}^{am}Si_4O_8$$
$$\quad\quad an \quad\quad\quad\quad\quad qz$$

$$+ [2(X_{an}^{am} - a_{an}^{am}) - 1.33(X_{an}^{am} - a_{an}^{am})/2]/$$

$$1.455\ Al_{1.455}Si_{2.91}O_8$$
$$\quad\quad dpy$$

$$+ (X_{an}^{am} - a_{an}^{am})/2.0\ Ca_2Al_{1.33}Si_2O_8. \quad (10)$$
$$\quad\quad\quad\quad gr$$

The quantification of the effect of pressure on $X_{an}^{am} - a_{an}^{am}$ in this system involved the assumption that this reaction was the sole contributor to the lowering of a_{an}^{am} and a_{qz}^{am} in the compositional range $X_{an}^{am} \leq X_{an}^{am}(E)$. This assumption necessitated, in turn, the assumption that the a_{an}^{am} and a_{qz}^{am} relationship in Reaction 10 was maintained at pressures below 14 kbar, permitting calculation of the eutectic compositions.

Investigation of the variation of $X_{an}^{am} - a_{an}^{am}$ and $X_{qz}^{am} - a_{qz}^{am}$ in the H₂O-saturated An-Qz binary from 1 bar to 10 kbar was conducted along the univariant melting curve of Stewart (1967). The eutectic compositions determined by Stewart (1967) permit an independent check on the proposed speciation reaction in this system. When the a_{an}^{hm} and a_{qz}^{hm} are converted onto an anhydrous basis (Eq. 3–6) and inserted into Equation 10, the resulting eutectic compositions show excellent agreement (within the stated experimental error) with those determined experimentally by Stewart (1967)! As in the case of the binary Ab-Qz, this agreement indicates that the proposed reaction in the anhydrous system An-Qz is reasonable and that, although the addition of H₂O to the system increases the extent of speciation, the nature of the speciation reaction is not significantly affected.

Speciation by dissociation in sanidine ($KAlSi_3O_8$) melts. The cryoscopic equation for sanidine was used to investigate the degree of speciation, $X_{or}^{am} - a_{or}^{am}$, along the anhydrous melting curve of sanidine (Boettcher et al., 1984). The variation of $X_{or}^{am} - a_{or}^{am}$ exhibits a slight decrease in the degree of dissociation with increasing pressure. This behavior was anticipated, because sanidine, in contrast to the other feldspars, melts incongruently at 1 bar, but congruently above approximately 15 kbar (Boettcher et al., 1984) or 18 kbar (Lindsley, 1966). It is reasonable to assume, therefore, that at pressures below the singular point, a leucite-like melt species is formed.

Along the H₂O-saturated solidus, at H₂O pressures above 4 kbar, it is assumed that there is no dissociation of sanidine (i.e., $X_{or}^{am} - a_{or}^{am} = 0.0$). This assumption permitted the derivation of a cryoscopic equation for sanidine. However, at H₂O pressures

below 2.6 kbar, Goranson (1938) indicated that sanidine exhibits incongruent behavior. Inasmuch as this incongruency once again resulted in the formation of Lc + L, it is reasonable to suppose that this results in the formation of *lc* and *qz* in the melt.

Speciation by interaction in the system KAlSi$_3$O$_8$-Si$_4$O$_8$-H$_2$O. The effect of *qz* on sanidine melts was evaluated by computing a_{or}^{am} and a_{qz}^{am} along the Or + Qz $\rightleftharpoons$ L univariant curve of Bohlen et al. (1983). These investigators did not determine the eutectic compositions at the pressures of their investigation, but Boettcher (1982, pers. comm.) obtained an estimate of the eutectic composition at 15 kbar. The activities of the components *or* and *qz,* calculated at 15 kbar (1443 K), when combined with the compositional estimate of Boettcher (1982, pers. comm.), yields the reaction
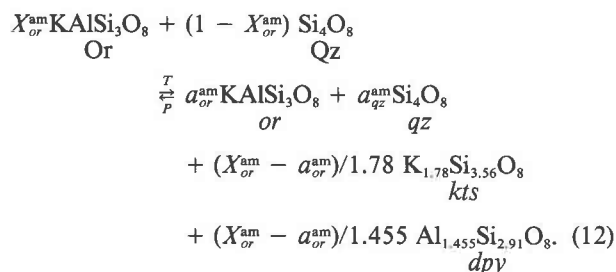
$$0.773 \underset{\text{Or}}{\text{KAlSi}_3\text{O}_8} + 0.227 \underset{\text{Qz}}{\text{Si}_4\text{O}_8}$$

$$\underset{\text{15 kbar}}{\overset{\text{1443 K}}{\rightleftharpoons}} 0.329 \underset{or}{\text{KAlSi}_3\text{O}_8} + 0.117 \underset{qz}{\text{Si}_4\text{O}_8}$$

$$+ 0.249 \underset{kts}{\text{K}_{1.78}\text{Si}_{3.56}\text{O}_8}$$

$$+ 0.305 \underset{dpy}{\text{Al}_{1.455}\text{Si}_{2.91}\text{O}_8}, \quad (11)$$
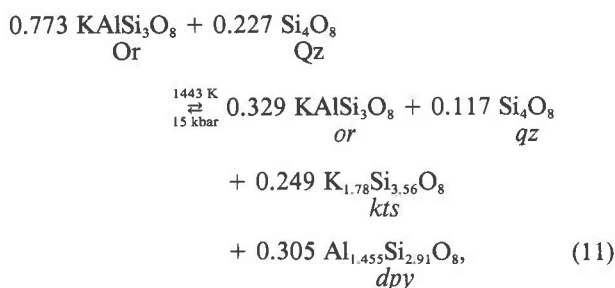
which results in the formation of potassium tetrasilicate (*kts*) and *dpy*.

In order to compare this reaction with one postulated for the H$_2$O-saturated system, Or-Qz-H$_2$O, a_{or}^{am} and a_{qz}^{am} were calculated along the Or + Qz (+ H$_2$O) $\rightleftharpoons$ L (+ V) curve of Shaw (1963) at 1–4 kbar and along the higher-pressure extension of Lambert et al. (1969). Shaw (1963) was able to determine the eutectic compositions in the low-pressure region, providing compositional data that can be used to test the speciation reaction proposed. At the pressures and temperatures of Shaw's (1963) experiments, a_{or}^{am} and a_{qz}^{am}, converted to an anhydrous basis through use of Equations 3–6, were inserted into the reaction

$$X_{or}^{am}\underset{\text{Or}}{\text{KAlSi}_3\text{O}_8} + (1 - X_{or}^{am}) \underset{\text{Qz}}{\text{Si}_4\text{O}_8}$$

$$\overset{T}{\underset{P}{\rightleftharpoons}} a_{or}^{am}\underset{or}{\text{KAlSi}_3\text{O}_8} + a_{qz}^{am}\underset{qz}{\text{Si}_4\text{O}_8}$$

$$+ (X_{or}^{am} - a_{or}^{am})/1.78 \underset{kts}{\text{K}_{1.78}\text{Si}_{3.56}\text{O}_8}$$

$$+ (X_{or}^{am} - a_{or}^{am})/1.455 \underset{dpy}{\text{Al}_{1.455}\text{Si}_{2.91}\text{O}_8}. \quad (12)$$

The resulting calculated eutectic compositions exhibit excellent agreement (within the stated experimental error) with the compositional data of Shaw (1963); hence, this reaction was assumed at the eutectics at the higher pressures investigated by Lambert et al. (1969). This assumption permitted the calculation of eutectic compositions in

the H$_2$O-saturated system Or-Qz-H$_2$O at pressures above 4 kbar and, hence, the quantification of the pressure dependence of $X_{or}^{am} - a_{or}^{am}$ and $X_{qz}^{am} - a_{qz}^{am}$, via the stoichiometric relations in Reaction 12.

Quantification of the $X_i^{am} - a_i^{am}$ relations

In view of the fact that the difference $X_i^{am} - a_i^{am}$ is attributed to dissociation or interaction of component *i,* the stoichiometry of the speciation reaction over the entire composition range can be preserved only through the principle of mass action. Thus, in the case of dissociation, the compositional dependence of $X_i^{am} - a_i^{am}$ is simply reduced to X_i^{am}, whereas in the case of binary interaction, it is formalized by the product of the interacting-component mole fractions, $X_i^{am} \cdot X_j^{am}$. In this latter case, moreover, an additional constraint[9] arises from the fact that $X_i^{am} - a_i^{am}$ for only one of the interacting components can vary independently; $X_j^{am} - a_j^{am}$ is constrained to vary with $X_i^{am} - a_i^{am}$ in accordance with the stoichiometry of the speciation reaction. In Reaction 12, for example, equating the coefficients of the reactants with those of the products yields $X_{qz}^{am} - a_{qz}^{am} = 0.249 (X_{or}^{am} - a_{or}^{am})$ (Table 2c).

The $X_i^{am} - a_i^{am}$ relations have been quantified in such a way as to ensure continuity in all subsystems of the system Ab-An-Or-Qz-H$_2$O. For *qz,* which does not dissociate, any $X_{qz}^{am} - a_{qz}^{am} > 0$ must be the result only of interaction with aluminosilicate components. Thus, if a reaction can be identified at the eutectics of the A-Qz binaries at every pressure, then it follows that, in the composition region between $X_a^{am} \leq X_a^{am}(E)$ and $X_{qz}^{am} = 1.0$, the identified reaction is, indeed, the sole determinant of the relationship between $X_{qz}^{am} - a_{qz}^{am}$ and $X_a^{am} - a_a^{am}$. Quantification of the variations in $X_a^{am} - a_a^{am}$ in this compositional region, therefore, results in simple functions of pressure, weighted by the products of the mole fractions. Similar functions are obtained for the H$_2$O-saturated Qz-bearing ternaries, and the two sets of functions are linked under the assumption that $X_i^{am} - a_i^{am}$ is linearly dependent upon X_w^m. This assumption is dictated by the lack of reliable equilibrium data in H$_2$O-undersaturated hydrous systems. These functions, as well as an expression for $X_a^{am}(E)$, are presented in Tables 2b and 2a, respectively. Table 2c contains expressions for $X_{qz}^{am} - a_{qz}^{am}$.

Variations in $X_a^{am} - a_a^{am}$ in the compositional range $X_a^{am} > X_a^{am}(E)$ are more complex to quantify, because dissociation of *a* prevents $X_a^{am} - a_a^{am}$ from approaching zero as $X_{qz}^{am} \to 0.0$ in the A-Qz-(H$_2$O) systems. As a consequence, the expressions for $X_a^{am} - a_a^{am}$ embody the combined effects of dissociation and interaction, which are inseparable in this compositional region. The compositional dependence of $X_a^{am} - a_a^{am}$ is particularly complicated for the *or* component, which exhibits a peritectic relationship in Qz-bearing systems at low pressures. For-

---

[9] This constraint was not imposed by Burnham (1981), because the cryoscopic equations used in the earlier work were not sufficiently refined to permit identification of a single dominant speciation reaction over a large pressure range.

Table 2a. Change in eutectic composition with pressure and X_w^m for the A-Qz binaries: $X_a^{am}(E) = a + bP + cP^2 - (X_w^m/X_w^m \text{sat.})/[d + eP + fP^2]$; $P \equiv$ pressure in kilobars, $X_w^m \text{sat.} \equiv$ saturation mole fraction of H_2O calculated from Equations 3–6

Component a	Pressure Conditions	Coefficients					
		a	b	c	d	e	f
$\underline{ab}$	($\underline{P} < 1.0$)	0.670	0.023	-7.36×10^{-4}	0.000	0.101	-7.36×10^{-4}
	($\underline{P} \geq 1.0$)	0.670	0.023	-7.36×10^{-4}	0.104	-4.00×10^{-3}	5.56×10^{-4}
	($\underline{P} < 1.0$)	0.286	0.025	-3.50×10^{-4}	-0.1084	0.198	-6.18×10^{-4}
$\underline{an}$	($1.0 < \underline{P} \leq 12.0$)	0.286	0.025	-3.50×10^{-4}	0.080	-0.021	1.74×10^{-3}
	($\underline{P} > 12.0$)	0.198	0.033	-3.34×10^{-4}	0.080	-0.021	1.74×10^{-3}
$\underline{or}$	($\underline{P} \leq 1.0$)	0.617	0.016	-3.54×10^{-4}	0.00	0.087	-3.54×10^{-4}
	($\underline{P} > 1.0$)	0.617	0.016	-3.54×10^{-4}	0.084	9.19×10^{-3}	-3.91×10^{-4}

tunately, however, $X_a^{am} < X_a^{am}(E)$ in most multicomponent systems of petrologic interest; hence, these complex functions, which are presented in Table 2d, are relegated primarily to use in calculating binary or pseudobinary (with H_2O) liquidus relations.

Additional speciation reactions relevant to pegmatite compositions

Speciation by interaction in the system $NaAlSi_3O_8$-$KAlSi_3O_8$-Si_4O_8-$Al_{3.2}Si_{1.6}O_8$-H_2O. The extent of speciation of anorthite melts is two or more times that for albite melts. Consistent with this greater increase in $X_{an}^{am} - a_{an}^{am}$, anorthite melts incongruently to corundum (Al in sixfold coordination) plus qz-enriched melt at approximately 9.4 kbar (Hariya and Kennedy, 1968; Goldsmith, 1980), whereas albite melts incongruently to jadeite (Al in sixfold coordination) plus qz-enriched melt at approximately 32 kbar (Bell and Roseboom, 1969). In contrast, increasing the pressure on melts of sanidine ($KAlSi_3O_8$) composition causes $X_{or}^{am} - a_{or}^{am}$ to decrease and sanidine, which melts incongruently to leucite (Al in fourfold coordination) plus qz-enriched melt at atmospheric pressure, melts congruently at pressures greater than 15 (Boettcher et al., 1984) to 18 kbar (Lindsley, 1966). Thus, the consistency among these contrasting relationships strongly suggests, as proposed by Burnham (1979a, 1979b, 1981), that increasing the pressure on melts of albite and anorthite composition, but not on melts of sanidine composition, promotes dissociation in response to a shift from fourfold to higher coordination of at least part of the Al in the melts.

If, indeed, part of the Al in aluminosilicate melts is in sixfold coordination and part is in fourfold coordination, as in the feldspars, then there are sound theoretical reasons to presume that some of the Al also will be in intermediate, fivefold coordination. Accordingly, the evidence, some of which is presented below, strongly suggests that speciation in silica-rich melts (Si:Al > 2) commonly involves formation of a stable complex whose stoichiometry and structure mimic those of dehydroxylated pyrophyllite (dpy, $Al_{1.455}Si_{2.91}O_8$) in which all Al is in fivefold coordination (Wardle, 1972; Burnham, 1981, Fig. 9.5).

The necessity to invoke the presence of the dpy (Si:Al = 2:1) component in order to account for the $X_i^{am} - a_i^{am}$ relations and, at the same time, to balance several anhydrous, as well as hydrous, speciation reactions was cause for concern in the original formulation of the quasi-crystalline model (Burnham, 1981). This concern arose over the fact that dehydroxylated pyrophyllite is not a stable phase in any of the anhydrous aluminosilicate systems investigated thus far; the stable compositional equivalent, instead, is the assemblage quartz plus sillimanite, kyanite, or andalusite, in all three of which Si:Al = 1:2 (cf. Eq. 14). In hydrous systems, on the other hand, the structural analogue of pyrophyllite is muscovite (paragonite), which can be formed from pyrophyllite by replacing one-fourth of the Si^{4+} with $(K,Na)Al^{4+}$. A species with the stoichiometry of muscovite ($K_{0.72}Al_{2.18}Si_{2.18}O_8 \cdot 0.727 H_2O$; Si:Al = 1:1), however, cannot satisfy the $X_i^{am} - a_i^{am}$ relations in the system $KAlSi_3O_8$-Si_4O_8-H_2O, even at pressures and temperatures within the stability field of muscovite. Thus, it was proposed that muscovite dissolves in granitic melts by the reaction

Table 2b. Activity-composition relations for an, ab, or: $X_a^{am} - a_a^{am} = X_a^{am} X_{qz}^{am} \{a + bP + cP^2 - X_w^m/X_w^m(\text{sat.})[d + eP + fP^2]\}$ for $X_a^{am} \leq X_a^{am}(E)$, $X_{qz}^{am} > 0.0$; $P \equiv$ pressure in kilobars

Component a	Pressure Conditions	Coefficients					
		a	b	c	d	e	f
$\underline{ab}$	($\underline{P} < 3.0$)	0.1557	0.1868	-5.073×10^{-3}	0.6025	-0.3616	0.0423
	($\underline{P} > 3.0$)	0.1557	0.1868	-5.073×10^{-3}	-0.0712	-0.0313	7.057×10^{-3}
$\underline{an}$	($\underline{P} \leq 12.0$)	9.461×10^{-3}	-0.0215	4.543×10^{-3}	-0.7968	-0.2110	0.0140
	($\underline{P} > 12.0$)	-0.0535	-0.0738	9.339×10^{-3}	-0.7968	-0.2110	0.0140
$\underline{or}$	($\underline{P} \leq 10.0$)	1.153	0.1423	-3.362×10^{-3}	0.2168	0.0616	1.099×10^{-3}

Table 2c.   Activity-composition relations for qz: $X_{qz}^{am} - a_{qz}^{am} = \sum_a b(X_a^{am} - a_a^{am})^*$ for $X_a^{am} \leq X_a^{am}(E)^{**}$

Component a	Coefficient b
ab	0.083
an	0.418
or	0.249

*expression for $\underline{X}_a^{am} - \underline{a}_a^{am}$ ($\underline{P}$, $\underline{X}_w^m$, $\underline{X}_{qz}^m$) in Table 2b.

**although these expressions for $\underline{X}_{qz}^{am} - \underline{a}_{qz}^{am}$ are strictly valid only for the composition range $\underline{X}_a^{am} \leq \underline{X}_a^{am}(E)$, they can be used to obtain an estimate of the metastable quartz liquidus temperatures, in the range $\underline{X}_a^{am} > \underline{X}_a^{am}(E)$.

$$K_{0.727}Al_{2.18}Si_{2.18}O_8 \cdot 0.727 \, H_2O + 0.727 \, Si_4O_8$$
$$\text{muscovite} \qquad\qquad\qquad\qquad qz$$

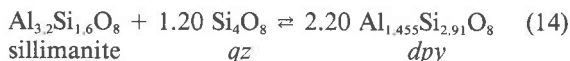$$\rightleftharpoons Al_{1.455}Si_{2.91}O_8 \cdot 0.727 \, H_2O$$
$$py$$

$$+ \, 0.727 \, KAlSi_3O_8, \qquad (13)$$
$$or$$
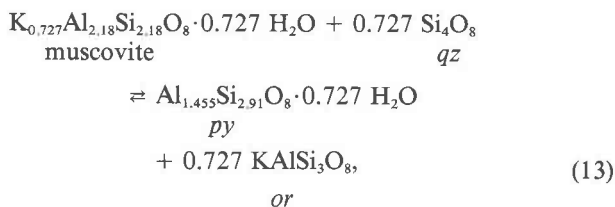
where *py* is the hydroxylated analogue of *dpy*. Similarly, under conditions where muscovite is not stable, one of its reaction products, sillimanite, was hypothesized to dissolve by the reaction

$$Al_{3.2}Si_{1.6}O_8 + 1.20 \, Si_4O_8 \rightleftharpoons 2.20 \, Al_{1.455}Si_{2.91}O_8 \quad (14)$$
$$\text{sillimanite} \qquad\quad qz \qquad\qquad\qquad dpy$$

from which it is apparent that, if the reaction proceeds to completion, 1.20 mol of *qz* component will be consumed in producing *dpy* species for every mole of sillimanite dissolved.

To test this reaction scheme, hence the existence of *dpy*, Voigt (1983) conducted experiments to determine the effects on the sanidine and quartz liquidi of dissolving 3.5 mol% sillimanite in melts of the system $KAlSi_3O_8(or)$-$Si_4O_8(qz)$-H_2O at a pressure of 2.0 kbar. Before saturating the melts with sillimanite, the sanidine-quartz eutectic, projected onto the anhydrous join, was located at $X_{or}^{am} = 0.544$, $X_{qz}^{am} = 0.456$, and 767°C, in excellent agreement with the experimental results of Shaw (1963). Upon saturation with sillimanite ($X_{sil}^{am} = 0.035$), however, the eutectic, projected onto the anhydrous $KAlSi_3O_8$-Si_4O_8 join, was found to have shifted to $X_{or}^{am} = 0.524\pm0.01$, $X_{qz}^{am} = 0.476\pm0.01$, and 737 ± 5°C. Moreover, the sanidine liquidus boundary at the original eutectic temperature (767°C) was found not to have shifted perceptibly in projected composition, but the quartz liquidus boundary shifted between 4% and 5% toward Si_4O_8. This shift is well within the limits of experimental error of that calculated from Equations 3–6 and those in Tables 1 and 2, on the assumption that the reaction
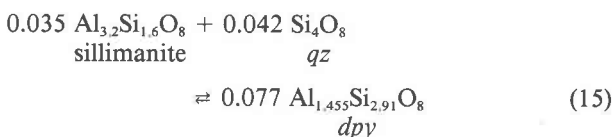
$$0.035 \, Al_{3.2}Si_{1.6}O_8 + 0.042 \, Si_4O_8$$
$$\text{sillimanite} \qquad\qquad\quad qz$$

$$\rightleftharpoons 0.077 \, Al_{1.455}Si_{2.91}O_8 \qquad (15)$$
$$dpy$$

Table 2d.   Expressions for $X_a^{am} - a_a^{am}$ [$X_{qz}^{am} = 0.0$, $X_a^{am} > 0$ or $X_{qz}^{am} > 0.0$, $X_a^{am} > X_a^{am}(E)$]

$$\underline{X}_{ab}^{am} - \underline{a}_{ab}^{am} = \underline{X}_{ab}^{am} \begin{cases} [(\underline{P} \leq 14.0) \, 0.0362\underline{P} - 2.152\times10^{-3}\underline{P}^2 + 4.097\times10^{-5}\underline{P}^3] \\ [(\underline{P} > 14.0) \, 0.1944 - 1.746\times10^{-4}\underline{P} + 2.822 \times 10^{-5}\underline{P}^2] \end{cases}$$

$$- \underline{X}_w^m/\underline{X}_w^m \text{sat.} \begin{cases} [(\underline{P} < 2) \, 0.0362\underline{P} - 2.152\times10^{-3}\underline{P}^2 + 4.097\times10^{-5}\underline{P}^3] \\ [(\underline{P} > 2) \, 0.1792 - 0.0690\underline{P} + 5.148\times10^{-3}\underline{P}^2 + 4.097\times10^{-5}\underline{P}^3] \end{cases}$$

$$+ \underline{X}_{ab}^{am} \, \underline{X}_{qz}^{am} \begin{cases} [(\underline{P} \leq 10.0) \, 0.3474 + 9.52\times10^{-4}\underline{P}^2] \\ [(\underline{P} > 10.0) \, 0.3842 + 0.0106\underline{P} - 4.712\times10^{-4}\underline{P}^2] \end{cases}$$

$$- \underline{X}_w^m/\underline{X}_w^m \text{sat.} \begin{cases} [(\underline{P} \leq 3) \, 0.9878 - 0.8388\underline{P} + 0.1452\underline{P}^2] \\ [(\underline{P} > 3) - 0.4587 + 0.1010\underline{P} - 8.178\times10^{-3}\underline{P}^2] \end{cases}$$

$$\underline{X}_{an}^{am} - \underline{a}_{an}^{am} = \underline{X}_{an}^{am} \begin{cases} [0.0326\underline{P} - 1.244\times10^{-4}\underline{P}^2] \end{cases}$$

$$- \underline{X}_w^m/\underline{X}_w^m \text{sat.} \begin{cases} [0.0604\underline{P} - 0.0187\underline{P}^2 + 1.192\times10^{-3}\underline{P}^3] \end{cases}$$

$$+ \underline{X}_{an}^{am} \, \underline{X}_{qz}^{am} \begin{cases} [(\underline{P} \leq 12) - 0.0062 - 0.0607\underline{P} + 2.290\times10^{-3}\underline{P}^2] \\ [(\underline{P} > 12) - 1.643 + 0.1310\underline{P} - 2.320\times10^{-3}\underline{P}^2] \end{cases}$$

$$- \underline{X}_w^m/\underline{X}_w^m \text{sat.} \begin{cases} [- 0.9836 - 0.1579\underline{P} + 0.0117\underline{P}^2] \end{cases}$$

$$\underline{X}_{or}^{am} - \underline{a}_{or}^{am} = \underline{X}_{or}^{am} \begin{cases} [0.3317 - 9.966\times10^{-3}\underline{P} + 2.04\times10^{-4}\underline{P}^2] \end{cases}$$

$$- \underline{X}_w^m/\underline{X}_w^m \text{sat.} \begin{cases} [(\underline{P} \leq 3) \, 0.1006\underline{P} + 2.040\times10^{-4}\underline{P}^2] \\ [(\underline{P} > 3) \, 0.3317 - 9.966\times10^{-3}\underline{P} + 2.040\times10^{-4}\underline{P}^2] \end{cases}$$

$$+ FQZ^* - \underline{X}_w^m/\underline{X}_w^m \text{sat.} \cdot \left\{ FQZ - \underline{X}_{or}^{am} \cdot \underline{X}_{qz}^{am} \begin{cases} [(\underline{P} \leq 3) \, 0.2869 + 0.2917\underline{P} - 2.680\times10^{-3}\underline{P}^2] \\ [(\underline{P} > 3) \, 1.223 - 0.0198\underline{P} + 0.0027\underline{P}^2] \end{cases} \right\}$$

*$FQZ = \underline{X}_{or}^{am} [702.1 \, \underline{X}_{qz}^{am9} + 1.586 \, \underline{X}_{qz}^{am3} \cdot \underline{P} + 0.2551 \, \underline{X}_{qz}^{am4} \cdot \underline{P}^2 - 0.1811 \, \underline{X}_{qz}^{am6} \cdot \underline{P}^3]$

proceeds to completion and a_{qz}^{am} is reduced by 0.042 as a result of complexing. Complete conversion of all *sil* to *dpy* (*py*) is not possible, of course, but the results are virtually unequivocal in establishing the existence of a melt species with the stoichiometry of *dpy* and in demonstrating that the *dpy* complex is very much more stable than the *sil* complex in *qz*-rich melts, in accordance with the principle of mass action. The experimental results also preclude the existence of a muscovite-like species in significant amounts, even in peraluminous melts, because the dissolution of sillimanite has no discernible effect on the sanidine liquidus, hence on a_{or}^{am}, except that of dilution.

Similarly, Joyce (1985) experimentally determined the effects of saturating melts in the system $NaAlSi_3O_8$-Si_4O_8-H_2O at 2.0 kbar with 3.5% sillimanite. Again, the dissolution of sillimanite affected the albite liquidus only to the extent of dilution, whereas the quartz liquidus at the albite-quartz eutectic temperature (750 ± 5°C) was again shifted between 4% and 5% toward Si_4O_8. The albite-quartz eutectic, in projection, also shifted from $X_{ab}^{am} = 0.615$ to $X_{ab}^{am} = 0.585$ and down in temperature to 735 ± 5°C. These results thus confirm the findings from the *or*-bearing system regarding the mechanism of solution of sillimanite and the relative stability of the *dpy* (*py*) complex. Together, these results on the system $NaAlSi_3O_8$-$KAlSi_3O_8$-Si_4O_8-$Al_{3.2}Si_{1.6}O_8$-H_2O also give new insights, which will be discussed in a subsequent section, into melting and crystallization processes in peraluminous granitic magmas.

Speciation by interaction in the system NaAlSi₃O₈(ab)-Si₄O₈(qz)-Li₂Al₂Si₂O₈(eu)-H₂O. The effects of melt speciation on liquidus relations just described, although important to a quantitative understanding of phase relations in granitic magmas, are relatively small compared to the effects in the system $NaAlSi_3O_8(ab)$-$Si_4O_8(qz)$-$Li_2Al_2Si_2O_8(eu)$-H_2O. Thus, according to Stewart (1978, Fig. 4), whose experimental results at 2.0-kbar P_{H_2O} are shown in Figure 3, dissolution of 16.8 mol% eucryptite in melts of the system $NaAlSi_3O_8$-Si_4O_8-H_2O causes a shift in the field boundary between quartz and albite from $X_{qz}^{am} = 0.385$ and $X_{ab}^{am} = 0.615$ to $X_{qz}^{am} = 0.509$, $X_{ab}^{am} = 0.323$, and $X_{eu}^{am} = 0.168$; at this composition, quartz and albite are joined by petalite ($Li_{0.8}Al_{0.8}Si_{3.2}O_8$) at a eutectic. As X_{qz}^{am} increases along this boundary, moreover, the temperature[10] of the quartz liquidus actually decreases from 750°C to 655°C—a behavior that is contrary to thermodynamic reason, unless a_{qz}^{am} is lowered by a speciation reaction that consumes a large proportion of the Si_4O_8 component. That such a speciation reaction does occur in the presence of $Li_2Al_2Si_2O_8$ is evident from the fact that $X_{qz}^{am} - a_{qz}^{am} = 0.00$ at the albite-quartz eutectic, whereas it is 0.252 at $X_{eu}^{am} = 0.168$ (the eutectic).

The identity of the lithium aluminosilicate species that consumes all of this Si_4O_8 is further evident from the fact that petalite is present at the eutectic and the stoichiometry of the reaction

$$0.168\ Li_2Al_2Si_2O_8 + 0.252\ Si_4O_8$$
$$eu \qquad\qquad qz$$

$$\rightleftarrows 0.420\ Li_{0.8}Al_{0.8}Si_{3.2}O_8. \qquad (16)$$
$$pe$$
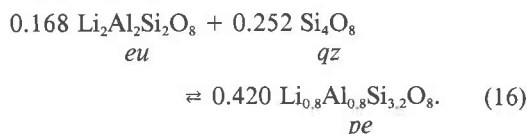
The fact that the amount of qz consumed (25.2 mol%) is precisely that required to convert all of the eu to pe within the limits of experimental error in composition ($\pm 1.0\%$) implies that very little of either eu or a spodumene-like ($Li_{1.33}Al_{1.33}Si_{2.67}O_8$, sp) species is present in this eutectic melt at 2.0 kbar. It also implies that the $Li_{0.8}Al_{0.8}Si_{3.2}O_8$ (pe) component mixes essentially ideally with the Si_4O_8 and $NaAlSi_3O_8$ components, and, as a consequence, with the $KAlSi_3O_8$ component, as well (Burnham et al., 1978; Lasaga and Burnham, 1979).

The ideal mixing behavior of ab and pe is confirmed by the albite liquidus relations along the join albite-petalite, which is shown in Figure 3b, replotted from Figure 3a. At the intersection of the 750°C isotherm with this join, for example, $X_{ab}^{am} = 0.585$—precisely the value of a_{ab}^{am} calculated from Equations 3–6 and those in Tables 1 and 2. Thus, ab not only mixes ideally with pe at this point, it does not speciate ($X_{ab}^{am} - a_{ab}^{am} = 0.0$). This lack of speciation does not hold, however, along either the albite-spodumene or albite-eucryptite joins, as is evident in Figure 3a from the fact that the 750°C isotherm intersects
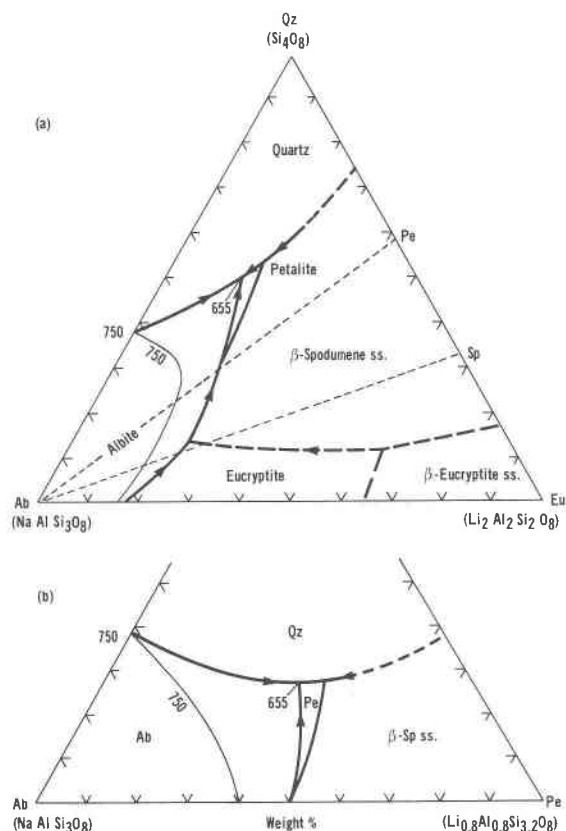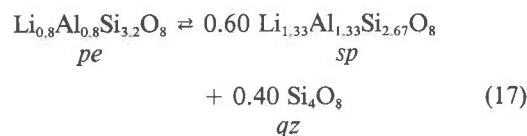

Fig. 3. Liquidus relations in the systems (a) Ab-Qz-Eu-H₂O, modified from Stewart (1978), and (b) Ab-Qz-Pe-H₂O, replotted from (a), at $P_{H_2O} = 2.0$.

these joins at successively higher values of X_{ab}^{am}. In other words, speciation of the relatively silica-rich ab component to produce more silica-rich lithium aluminosilicate species increases with decreasing silica content of the Li-bearing component.

Although the liquidus phase relations in the system of Figure 3 have not been investigated experimentally at higher H₂O pressures, the lithium aluminosilicate phase relations determined by London (1984), coupled with the experimentally determined melting relations of the Harding, New Mexico pegmatite by Burnham and Jahns (1962) and Vaughan (1963), indicate that petalite is replaced by spodumene + quartz at $P_{H_2O} > 3.5$–4.0 kbar and eutectic temperatures. These same melting relations, which will be discussed at greater length in a subsequent section, further indicate that as pressure is increased above approximately 2 kbar, equilibrium in the speciation reaction

$$Li_{0.8}Al_{0.8}Si_{3.2}O_8 \rightleftarrows 0.60\ Li_{1.33}Al_{1.33}Si_{2.67}O_8$$
$$pe \qquad\qquad\qquad sp$$

$$+\ 0.40\ Si_4O_8 \qquad (17)$$
$$qz$$

shifts progressively and gradually to the right, but conversion is not complete below 10 kbar. In one important

---

[10] The temperature at this eutectic is here assumed to be 15°C higher than that reported by Stewart (1978, p. 976), because Stewart's "redetermined" albite-quartz eutectic temperature is 15°C lower (735°C) than that originally determined by Tuttle and Bowen (1958) and recently confirmed by Joyce (1985).
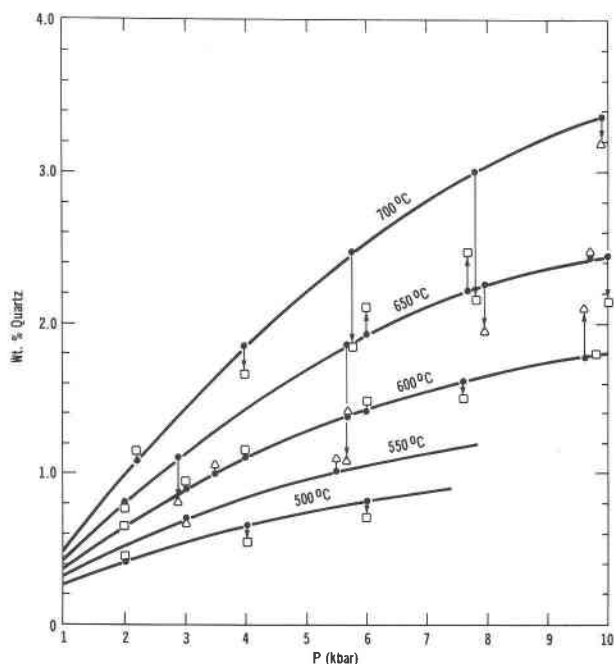
Fig. 4. Pressure and temperature dependence of the isothermal weight percent solubility of quartz in H_2O (curves) and normative quartz contents of aqueous fluids reacted with the Spruce Pine (JB-5, open squares) and Harding (JB-3, open triangles) pegmatites and their melts. Deviations from the solubility isotherms of Anderson and Burnham (1965) are indicated by arrows.

Fig. 5. Pressure and temperature dependence of the normative albite content of aqueous fluids in the system albite-H_2O (curves) and the normative total feldspar contents of aqueous fluids reacted with the Spruce Pine (JB-5, open squares) and Harding (JB-3, open triangles) pegmatites and their melts. Deviations from the normative albite isotherms of Davis (1972) are indicated by arrows.

respect, then, the *pe-sp* relationship is analogous to the *ab-jd* relationship in that the shift with pressure, in accordance with the quasi-crystalline model, stems from the same cause—a shift in Al coordination from fourfold (petalite, albite) to sixfold (spodumene, jadeite).

AQUEOUS FLUIDS IN PEGMATITE SYSTEMS

Aqueous-fluid compositions

The discussions in this section will focus on the results of experiments conducted with Dick Jahns on one sample each from the Harding pegmatite, Taos County, New Mexico, and the Spruce Pine pegmatite, Yancey County, North Carolina. The Harding sample (JB-3)—the chemical composition, CIPW norm, and component mole fractions of which are presented in Table 3—is the same composite diamond-drill core and mine chip sample used in the melting and H_2O solubility experiments of Burnham and Jahns (1962). The Spruce Pine sample (JB-5) is a composite grab sample collected by Dick Jahns (ca 1958) from the quarries of the Feldspar Corporation of Spruce Pine; its chemical composition, norm, and component mole fractions also are presented in Table 3.

The experiments were conducted in internally heated pressure vessels of the design described by Holloway (1971); in fact, these large-volume vessels were originally designed and constructed specifically for these experiments on aqueous-fluid compositions. The experimental charges, which generally consisted of approximately 3.0–4.0 g of pulverized pegmatite and 8–12 g of distilled
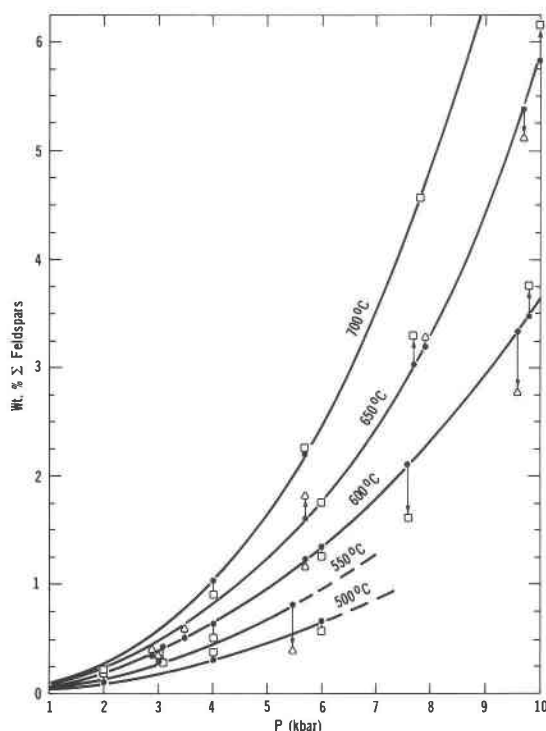
water, were contained in double gold capsules, precisely as described by Anderson and Burnham (1965). The experiments were run for 7 to 26 h at 500–900°C and 2.0–10 kbar.

After each experiment, the fluid phase, with quench precipitate, was removed from the large capsule and evaporated to dryness on mylar film. The residue was then analyzed by standard wet-chemical procedures that were adapted to small (≥ 100 mg) samples by C. O. Ingamells. The results of these analyses have been published in Clark (1966, Tables 19–18 and 19–19); hence, they will not be presented again here. Instead, the major oxides in the aqueous-phase residues have been recast into CIPW norms and are presented in summary form in Figures 4–6. [The normative mineral compositions of the Spruce Pine pegmatite fluids were previously presented in different format by Burnham (1967, Fig. 2.6, p. 49–57).]

In Figure 4, the normative quartz contents of fluids coexisting with the two pegmatite samples are shown in comparison with the quartz solubility isotherms from Anderson and Burnham (1965). Similarly, the normative total-feldspar (Ab + Or + An) contents are shown in Figure 5 relative to isotherms for the normative albite contents of fluids in the system albite-H_2O from Davis (1972). The remaining major normative constituents, spodumene (Sp) in the Harding fluids and sodium silicate (Ns) or corundum (Co) in both fluids, are plotted in Figure 6.

An examination of Figure 4 reveals that at temperatures of 600°C or lower there is generally excellent correspondence between the normative Qz content of the fluid and

the solubility of quartz in H_2O. The single major discrepancy is a strong positive deviation in a JB-3 sample at 9.6 kbar and 600°C. This same sample shows a strong negative deviation from the normative Ab isotherm in Figure 5, as well as a strong positive deviation from the normative Ns curve in Figure 6, which, incidentally, is essentially independent of temperature. Together, the directions and extents of these deviations clearly indicate that the discrepancy is a result of an erroneously low Al_2O_3 analysis. Similarly, the relatively small negative deviation from the 600°C quartz isotherm of the JB-5 sample at 7.6 kbar correlates with strong negative deviations in both total feldspar (Fig. 5) and Ns (Fig. 6), indicating an erroneously low total-alkali analysis. The remaining significant discrepancy in the 500–600°C temperature range is a negative deviation from the 550°C isotherm for normative albite in a JB-3 sample at 5.5 kbar, which is also accompanied by lower-than-expected normative spodumene; the cause of these latter discrepancies appears to be failure to attain equilibrium in this experiment.

Upon further examination of Figures 4 and 6, it becomes evident that several large negative deviations of JB-3 and JB-5 samples occur along the 650°C and 700°C isotherms, respectively. In every case, the deviations can be attributed to failure of the fluid phase to equilibrate with the bulk of the pegmatite sample in the inner capsule, because the pegmatite was either partially or completely molten (cf. Fig. 8). Upon melting, access of the aqueous fluid to the pegmatite sample was restricted to the very small volumes of melt in the vicinity of the pinholes in the inner capsules, and, because the ratio of normative quartz and spodumene to total feldspar in the aqueous phase was greater than in the bulk pegmatite melt, except at pressures near 10 kbar, selective leaching of *qz* and *sp* components occurred. As a consequence, the fluids equilibrated only locally with feldspar-bearing melts in which the activities (and mole fractions) of the *qz* and *sp* components had been substantially diminished over their values in the original pegmatite melt. The activities of the feldspar-like components, on the other hand, were unaffected; hence the normative total-feldspar contents remain essentially on the normative albite isotherms of Figure 5. The apparent retrograde solubility of spodumene (Fig. 6) and quartz (Fig. 4) over the intermediate pressure range is therefore an artifact of the experimental design. This same artifact of design appears to have plagued the experiments of Luth and Tuttle (1969).

The remaining significant deviations from the isotherms in Figures 4 and 5 are moderate positive deviations, which can be attributed to minor contamination of the aqueous-phase sample by material sifting out of the perforated inner capsule. The experimental limitations and analytical uncertainties considered, then, the data summarized in Figures 4–6 provide incontrovertible evidence that (1) 99% or more of the aqueous-phase solute can be recast in terms of the major mineral compositions in the coexisting pegmatite; (2) the remaining 1% or less of the solute appears as normative sodium silicate
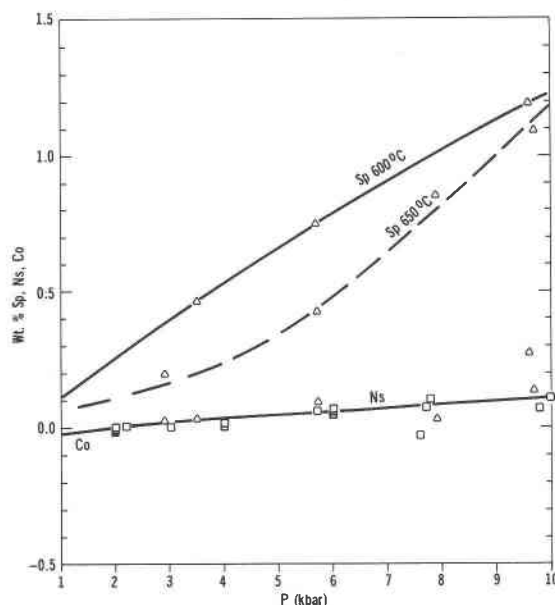

Fig. 6. Normative spodumene (Sp) content of aqueous fluids reacted with the Harding pegmatite (JB-3) and its melts, and the normative sodium silicate (Ns) or corundum (Co) contents of fluids reacted with both pegmatites and their melts (symbols as in Fig. 4).

$(Na_2Si_2O_5)$ in virtually the same proportions to normative Ab as in the system albite-H_2O (Davis, 1972); (3) in the presence of quartz or near the quartz liquidus, the normative Qz content of the aqueous fluid is equal to the solubility of quartz in H_2O at the same pressure and temperature (Anderson and Burnham, 1965), within the combined limits of experimental and analytical error; (4) in the presence of a feldspar or near the feldspar liquidus, the normative total-feldspar contents of the fluids are the same as the normative Ab content of the fluids in the system albite-H_2O (Davis, 1972), again within the combined limits of experimental and analytical error; and (5) the presence of spodumene in JB-3 merely increases the total solute content of JB-3 fluids by the amount of normative Sp present. These findings have an important bearing on the nature of speciation in magmatic aqueous fluids, as well as in coexisting silicate melts; hence, they will be explored more fully in the following paragraphs.

Aqueous-fluid speciation

The first finding enumerated above was first noted by Burnham (1967), who pointed out that total-silica contents of fluids in equilibrium with the Spruce Pine pegmatite far in excess of the solubility of quartz implied the existence of more than one form of aqueous silica. More recently, Anderson and Burnham (1983) suggested that, in addition to the H_4SiO_4 product of quartz dissolution, silica might be complexed with Al and an alkali to form an aqueous species with the stoichiometry of feldspar. This suggestion was based, in part, on the fact that the Al_2O_3 content of these fluids was many times the solubility

of corundum in H_2O (Anderson and Burnham, 1967). Now, with inclusion of the data on the Harding pegmatite in Figures 4–6, it is necessary to add to this list a stable complex with the stoichiometry of spodumene. In fact, the data in Figure 4 indicate that this aqueous species must be spodumene-like and not either petalite-like or eucryptite-like in stoichiometry under all pressure-temperature conditions where spodumene coexists with the fluid. If the Li-bearing species was petalite-like in stoichiometry, for example, the normative Qz contents of JB-3 samples in Figure 4 would lie 0.30 to 0.79 wt% below the 600°C quartz-solubility isotherm. Conversely, if the species was eucryptite-like, the normative Qz contents would lie 0.1 to 0.4 wt% above this isotherm. Thus, there appears to be little doubt that aqueous species with the stoichiometries of spodumene, the alkali feldspars,[11] and quartz constitute the bulk of the aqueous phase in equilibrium with the Harding and Spruce Pine pegmatites and their melts. In addition, a sodium silicate, presumably with the Si:Na stoichiometry of *nds* ($Na_{3.2}Si_{3.2}O_8$) or NaH_3SiO_4 (Anderson and Burnham, 1983), becomes increasingly abundant as pressure is increased, concomitant with the increasing stability of micas.

Despite the difficulty in visualizing the existence of large polynuclear aqueous complexes with feldspar stoichiometry, the evidence presented here for fluids in equilibrium with feldspars is compelling. The evidence, especially that presented in Figure 5, is equally compelling that these feldspar-like aqueous species persist, their concentrations virtually unaffected by the disappearance of feldspar, to temperatures above the feldspar liquidi. Moreover, the concentrations of the quartz-like species also are unaffected by the disappearance of quartz if due allowance is made for disequilibrium in some experiments, as discussed previously. Thus, even at temperatures above their respective liquidi, the feldspar-like and quartz-like aqueous species behave independently, a clear indication that the corresponding melt species also maintain their integrity. The experimental data on pegmatite aqueous-phase compositions, therefore, provide strong corroborative evidence for the quasi-crystalline melt speciation model.
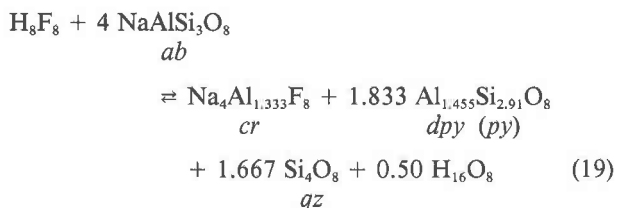
Speciation in the presence of other volatiles

Effects of chlorine. The addition of relatively small amounts of chlorine, as HCl, to the pegmatite-H_2O systems has profound effects on aqueous-phase compositions and, hence, on aqueous speciation (Burnham, 1967). These effects arise from the facts that the alkali chlorides form very stable complexes in aqueous fluids, Cl is relatively insoluble in peraluminous melts of granite composition, and, as a result, the partition coefficient for Cl is very large (~40) in favor of the aqueous phase (Kilinc and Burnham, 1972). Owing to the relatively greater stability of the alkali

chloride complexes, as compared with the large feldspar-like complexes just described, homogeneous aqueous-phase reactions of the type

$$NaAlSi_3O_{8(aq)} + HCl \rightleftharpoons NaCl_{(aq)} + 0.5\ Al_2O_{3(aq)} + 3\ SiO_{2(aq)} + 0.5\ H_2O \quad (18)$$
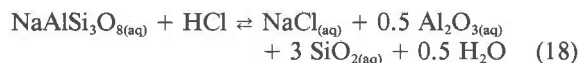
result in almost complete destruction of the feldspar-like aqueous species and concomitant fixation of an aluminous phase, such as corundum, one of the aluminum silicates, or a mica, all of which are highly insoluble in the aqueous phase (Anderson and Burnham, 1967, 1983). As a consequence, the normative feldspar content of aqueous-chloride solutions in equilibrium with these peraluminous pegmatite compositions drops to a value corresponding roughly to the solubility of corundum (cf. Burnham, 1967, Fig. 2.7). It should be emphasized, however, that these effects are for acidic, peraluminous granite compositions; highly peralkaline systems might well behave differently.
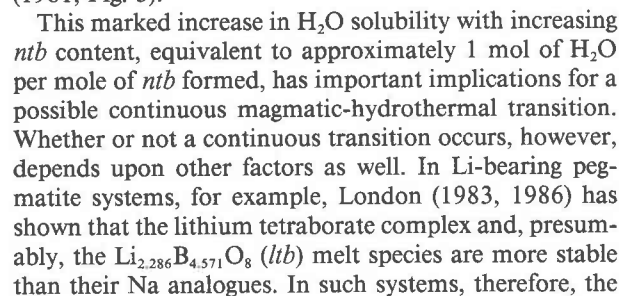
Effects of fluorine. In contrast to chlorine, fluorine is partitioned approximately 6:1 in favor of granitic melts (Hards, 1976); hence, the effects of F on aqueous-phase speciation are considerably less than on melt speciation. Manning (1981; cf. Manning and Pichavant, 1983), for example, found that addition of 1.0, 2.0, and 4.0 wt% F to the haplogranite system at $P_{H_2O} = 1.0$ kbar shifted the liquidus minimum to higher *ab* and lower *qz* contents, as shown in Figure 7. This compositional trend in the liquidus minimum with added F is opposite to that produced by the addition of H_2O ($X_w^m = 0.389$ at the saturated 1.0-kbar minimum) to the haplogranite system at constant pressure; hence, the solution of HF in granitic melts is not strictly analogous to the solution of H_2O—at least in the presence of H_2O—as presumed by Burnham (1979a, 1979b) and Manning and Pichavant (1983). Instead, the activity relationships for the *qz* component at the F-bearing liquidus minima calculated from Equations 3–6 and those in Tables 1 and 2 indicate that a speciation reaction with the stoichiometry of

$$H_8F_8 + 4\ NaAlSi_3O_8$$
$$ab$$

$$\rightleftharpoons Na_4Al_{1.333}F_8 + 1.833\ Al_{1.455}Si_{2.91}O_8$$
$$cr \qquad\qquad dpy\ (py)$$

$$+ 1.667\ Si_4O_8 + 0.50\ H_{16}O_8 \quad (19)$$
$$qz$$

is required to obtain agreement with the experimental temperatures and compositions; moreover, this reaction must proceed essentially to completion. Thus, the consumption of *ab* component to produce *cr*, a cryolite-like species, lowers a_{ab}^{am} and raises a_{qz}^{am}, causing not only a contraction of the albite liquidus field, but an expansion of the quartz liquidus field with only minor effect on the sanidine field. The fact that the sanidine liquidus is unaffected, except by dilution, supports the proposed speciation of *ab* to form *cr*, as does the occurrence of cryolite in some experimental products (Manning and Pichavant,

---

[11] So little normative anorthite is present in the fluids investigated (<0.02%) that the existence of an anorthite-like aqueous species is conjectural.

1983, p. 99). Also, the finding of Manning (1981) that the solubility of H_2O is not affected by the presence of F is confirmed by the activity-composition relations, which require that X_w^m be the same as in the absence of F at the same temperature and silicate composition. Similarly, the amounts by which the albite liquidus temperatures of Wyllie and Tuttle (1961, Fig. 3) are lowered upon addition of up to 12 wt% HF are within experimental error of those calculated on the assumption that Reaction 19 proceeds essentially to completion!

Application of these relationships to the F-bearing Harding pegmatite (0.64 wt% F) will be made in a subsequent section; here, however, it is appropriate to note that the cr-forming Reaction 19 has another significant implication for phase relations in F-bearing pegmatite magmas. In addition to the effects on a_{ab}^{am} and a_{qz}^{am}, cr formation also results in an increase in the activity of dpy (py) component, which in turn promotes stabilization of F-bearing muscovite (Eq. 13) or topaz, depending upon pressure. As a consequence, hypersolidus crystallization of either muscovite or topaz, which is the analogue of sillimanite in Reaction 14, tends to buffer the F content of residual pegmatite magmas and prevent, except rarely, the crystallization of primary cryolite.

Effects of boron. Like chlorine, boron partitions in favor of the magmatic aqueous phase, but only by a factor of 3:1 (Pichavant, 1981). Unlike Cl, however, B appears to form a stable aqueous complex predominantly with Na, as evidenced by strong enrichment of the aqueous phase in Na and concomitant impoverishment in Al relative to fluids in the B-free granite–H_2O system (Pichavant, 1981, Fig. 2). These results are consistent with an Al-free borate complex, probably with the stoichiometry of sodium tetraborate, $Na_2B_4O_7$, which also appears to be present in coexisting melts.

Pichavant (1984) added boron in the form of B_2O_3 to the haplogranite system at $P_{H_2O} = 1.0$ kbar and found that the liquidus minimum, as in the F-bearing system, shifted to lower temperatures and toward the Ab corner. As shown in Figure 7, the amount of shift away from the composition of the granite-H_2O minimum induced by 4.5 wt% B_2O_3 is approximately the same as for 1.0 wt% F, although the B-bearing minimum melts appear to be slightly richer in Qz and poorer in Or. The temperature of the 4.5% B_2O_3 melt minimum (660°C) also is approximately 30°C lower than the 1.0% F melt minimum, and according to Pichavant (1981, Fig. 3), the H_2O content of the B-bearing melt at saturation is slightly higher.

These changes in liquidus-phase relations are readily accounted for by the speciation reaction

$$H_8B_{2.667}O_8 + 1.333 \ NaAlSi_3O_8$$
$$ab$$

$$\rightleftarrows 0.583 \ Na_{2.286}B_{4.571}O_8 + 0.917 \ Al_{1.455}Si_{2.91}O_8$$
$$ntb \qquad\qquad dpy \ (py)$$

$$+ \ 0.333 \ Si_4O_8 + 0.50 \ H_{16}O_8 \qquad (20)$$
$$qz$$

Fig. 7. The haplogranite system at 1 kbar showing the effects of H_2O saturation on liquidus field boundaries, and the effects on liquidus minima of adding 1, 2, and 4 wt% F, as well as 4.5 wt% B_2O_3, to the haplogranite-H_2O system. The liquidous field boundaries were calculated using Equations 3–6 and those in Tables 1 and 2. The liquidus minima compositions and temperatures for F-bearing melts are from Manning and Pichavant (1983, Table 1), whereas the data for 4.5 wt% B_2O_3 are from Pichavant (1984).

to produce ntb, a sodium tetraborate–like species in which H_2O is more soluble than in the ab component from which it was formed. Like cr-forming Reaction 19, ntb formation consumes ab, thereby lowering a_{ab}^{am} and, hence, albite-liquidus temperatures for a given X_{ab}^{am}. As a consequence, the liquidus minimum shifts toward the Ab corner of Figure 7. The shift per mole of $H_8B_{2.667}O_8$ added is less pronounced than it is per mole of H_8F_8 added, however, because (1) only 0.33 as much ab is consumed, (2) only 0.2 as much qz is produced (cf. Reactions 19 and 20), and (3) increasing the H_2O content by a given amount preferentially depresses the quartz liquidus (cf. the slopes of the quartz- and feldspar-liquidus curves in Figs. 9 and 10). Thus, to achieve feldspar-quartz equilibrium at 660°C and 4.5 wt% B_2O_3 (Fig. 7), the thermodynamic relations presented in Equations 3–6 and those in Tables 1 and 3 indicate that X_w^m must be increased from 0.406 to 0.456, which is equivalent to 5.57 wt% H_2O and in excellent agreement with the experimental results of Pichavant (1981, Fig. 3).

This marked increase in H_2O solubility with increasing ntb content, equivalent to approximately 1 mol of H_2O per mole of ntb formed, has important implications for a possible continuous magmatic-hydrothermal transition. Whether or not a continuous transition occurs, however, depends upon other factors as well. In Li-bearing pegmatite systems, for example, London (1983, 1986) has shown that the lithium tetraborate complex and, presumably, the $Li_{2.286}B_{4.571}O_8$ (ltb) melt species are more stable than their Na analogues. In such systems, therefore, the

analogue of Reaction 20 involves consumption of *pe* or *sp* to produce *ltb, dpy (py)*, and *qz*. Both the *ltb*- and *ntb*-forming reactions, therefore, produce substantial amounts of *dpy (py)*, which promotes precipitation of tourmaline from peraluminous magmas. The precipitation of tourmaline, accompanied by quartz and perhaps albite, in turn tends to buffer the B content of residual pegmatite magmas and may inhibit the continuous transition from hydrous silicate melt to hydrothermal fluid. For this buffer to be effective, however, the bulk composition of the system should be markedly peraluminous, either initially or by later loss of alkalis to the wall rocks (Norton, 1983).

In summary, the precipitation from quartz-saturated pegmatite magmas of muscovite, sillimanite (andalusite, kyanite), topaz, spodumene, and tourmaline is accompanied in every case by the coprecipitation of quartz derived from either the *dpy* or *pe* components, or from both. When to this is added the quartz that precipitates from the generally more abundant *qz* component, it is not difficult to understand why zones in pegmatite bodies that are rich in these nonfeldspathic aluminosilicate minerals are also rich in quartz.

CRYSTALLIZATION OF THE SPRUCE PINE AND HARDING PEGMATITE MAGMAS

Experimental liquidus-solidus relationships

Pressure-temperature projections of the H_2O-saturated liquidi (L) and solidi (S) for the Spruce Pine (JB-5) and Harding (JB-3) pegmatites are presented in Figure 8. The JB-5L and JB-5S curves were determined experimentally by Vaughan (1963) and were presented previously by Burnham (1967, Fig. 2.3, "granite"). The JB-3S curve also was determined by Vaughan (1963), whereas the JB-3L curve was determined by Burnham and Jahns (1962, Fig. 3). These curves, which are presented together in Figure 8 for ease of comparison, strikingly illustrate the contrasting effects of the normative anorthite (An) content of JB-5, on one hand, and the normative spodumene (Sp) in JB-3, on the other (cf. Table 3).

At H_2O pressures up to 4.0 kbar along the JB-5L curve, plagioclase of undetermined composition (see below) is the liquidus phase. At higher pressures, however, the experimental results indicate that plagioclase is replaced by muscovite on the H_2O-saturated liquidus and, as a consequence, the muscovite liquidus takes on a nearly constant, positive slope of approximately $10°C \cdot kbar^{-1}$. This behavior, which results in a thermal minimum on the JB-5 liquidus, is fully consistent with the stability relations of muscovite at high P_{H_2O}.

A thermal minimum also occurs on the JB-3L curve, but for entirely different reasons. At pressures below 2.0 kbar, an alkali feldspar of undetermined composition (also see below) is the liquidus phase, whereas at higher pressures it is replaced by quartz; the quartz, in turn, is joined at still higher pressures by a white mica (Burnham and Jahns, 1962) that probably is a lithian muscovite. This anomalous positive slope of the quartz liquidus with increasing P_{H_2O}, hence increasing X_w^m, has been a long-stand-

ing enigma that only now finds ready explanation in the melt-speciation model. Thus, as discussed previously, the dominant lithium aluminosilicate species in JB-3 melts at 2.0 kbar (where the thermal minimum occurs) is *pe* ($Li_{0.8}Al_{0.8}Si_{3.2}O_8$), but upon increasing pressure there is a progressive shift in the *pe* decomposition equilibrium to produce more *sp* ($Li_{1.33}Al_{1.33}Si_{2.67}O_8$) and *qz* ($Si_4O_8$), in accordance with Reaction 17. The resulting increase in a_{qz}^m, in turn, is apparently more than enough to offset the decrease resulting from the increased X_w^m, thereby inducing a gradual rise in quartz-liquidus temperatures with increasing pressure. This same phenomenon, incidentally, prevents JB-3 solidus temperatures in Figure 8 from decreasing with increasing P_{H_2O} above 2.0 kbar, as they do for the Li-poor JB-5 composition.

Calculated phase relations

Phase-assemblage diagrams for the Spruce Pine and Harding pegmatite magmas have been calculated by the methods described by Nekvasil-Coraor and Burnham (1983, 1984)[12] using Equations 3–6 and those in Tables 1 and 2, and are shown in Figures 9 and 10. Owing to lack of reliable cryoscopic equations for sillimanite, the equilibrium properties of muscovite have not been calculated; instead, the muscovite-field boundary sketched in Figure 9b has been based on the experimental data in Figure 8. Similarly, cryoscopic equations for petalite and spodumene are presently lacking; hence, the field boundaries for these minerals sketched in Figures 10a and 10b are based on the experimental solidus results in Figure 8, as well as the observation by Stewart (1978) that the modal spodumene content of Li-rich pegmatites rarely, if ever, exceeds 25%. This spodumene content translates into an X_{pe}^{am} of 0.42, which is the petalite content of the eutectic mixture in Figure 3c and the basis of the argument (Stewart, 1978) for a magmatic origin of Li-rich pegmatites. Thus, the temperatures of first appearance of petalite or spodumene in Figures 10a and 10b are estimated as those at which $X_{pe}^{am} = 0.42$ ($X_{sp}^{am} = 0.25$). Also, for the purposes of these estimations, it is assumed that equilibrium with mica buffers the F content of H_2O-saturated JB-3 melts at the initial value (0.64 wt% F); as a consequence, the mole fraction of the *ab* component consumed in *cr*-forming Reaction 19 is held constant at 0.038.

The phase relations in Figures 9 and 10 are presented for 2.0 and 5.0 kbar primarily to illustrate the effects of pressure within a geologically reasonable framework. The occurrence of primary muscovite near the walls of the Spruce Pine pegmatite and of primary spodumene in the Harding pegmatite, however, indicate that these two pegmatites crystallized at pressures in excess of 3.0 and 3.5 kbar, respectively. Jahns and Ewing (1977) estimated that the depth of emplacement of the Harding pegmatite was

---

[12] The algorithms and source listing for the Fortran program PATH by which equilibrium-crystallization paths in haplogranitic systems can be calculated, are presented in Nekvasil (1985).
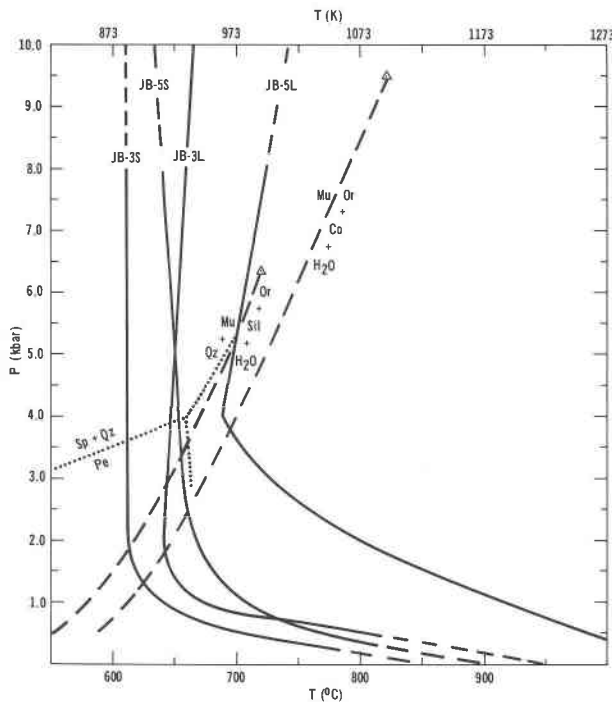
Fig. 8. Experimentally determined H_2O-saturated liquidus (L) and solidus (S) relations for the Spruce Pine (JB-5) and Harding (JB-3) pegmatites; the data for JB-5L, JB-5S, and JB-3S are from Vaughan (1963), whereas those for JB-3L are from Burnham and Jahns (1962). The Mu $\rightleftharpoons$ Or + Co + H_2O and Mu + Qz $\rightleftharpoons$ Or + Sil + H_2O curves (dashed) are from Chatterjee and Johannes (1974) and the Pe $\rightleftharpoons$ Sp + Qz boundary (dotted) is from London (1984).

Fig. 9. Phase-assemblage diagrams for the Spruce Pine pegmatite (JB-5) at (a) 2.0 kbar and (b) 5.0 kbar, calculated using Equations 3–6 and those in Tables 1 and 2, and the PATH program of Nekvasil-Coraor and Burnham (1984). Af = alkali feldspar, And = andalusite, L = liquid (melt), Mu = muscovite, Pl = plagioclase, Qz = quartz, Sil = sillimanite, and V = "vapor" (aqueous phase). The stability field of muscovite at 5.0 kbar is estimated from the experiments of Vaughan (1963).

in excess of 7 mi (>11 km), which is equivalent to approximately 3 kbar.

Spruce Pine pegmatite. The calculated phase relations in Figure 9 show that plagioclase is the liquidus phase in JB-5 melts at all P_{H_2O} values up to at least 9.0 kbar, and at 4.0 kbar the plagioclase-liquidus temperature is approximately 85°C above the first appearance of muscovite (Fig. 8). This apparently enormous discrepancy between the calculated and experimental liquidus relations is here attributed mostly to the failure of plagioclase to nucleate in unseeded, all-glass starting materials (cf. Erikson, 1979; Muncill, 1984; Swanson, 1977), even after a few days at temperature and pressure (Vaughan, 1963, Table 4).

The discrepancy between the calculated and experimental liquidus temperatures of JB-5 composition notwithstanding, the calculated H_2O-saturated solidi in Figures 9a and 9b are only 10–13°C below the experimentally determined JB-5S curve in Figure 8. Moreover, these calculations do not take into account the fact that the crystallization of either sillimanite (perhaps andalusite) at 2.0 kbar or muscovite at 5.0 kbar releases Si_4O_8 (cf. Reactions 19 and 18), which results in a slight increase in the temperature of the quartz field boundary. With due allowance for this effect, then, the agreement between the calculated and experimental solidi is excellent. Moreover, the fact

that the calculation of solidus relations proceeds through the calculation of liquidus relations and depends upon the proportions and compositions of phases previously crystallized suggests that the problem is, indeed, one of crystallization kinetics.

This agreement assumes special importance in the context of the present discussions, because the occurrence of very large crystals of plagioclase and muscovite near the margins of the Spruce Pine pegmatite imply that the magma reached saturation with H_2O fairly early in its crystallization history (Jahns and Burnham, 1969). Thus, assuming H_2O saturation, the first phase calculated to crystallize from JB-5 melt at 2.0 kbar (Fig. 9a) is plagio-
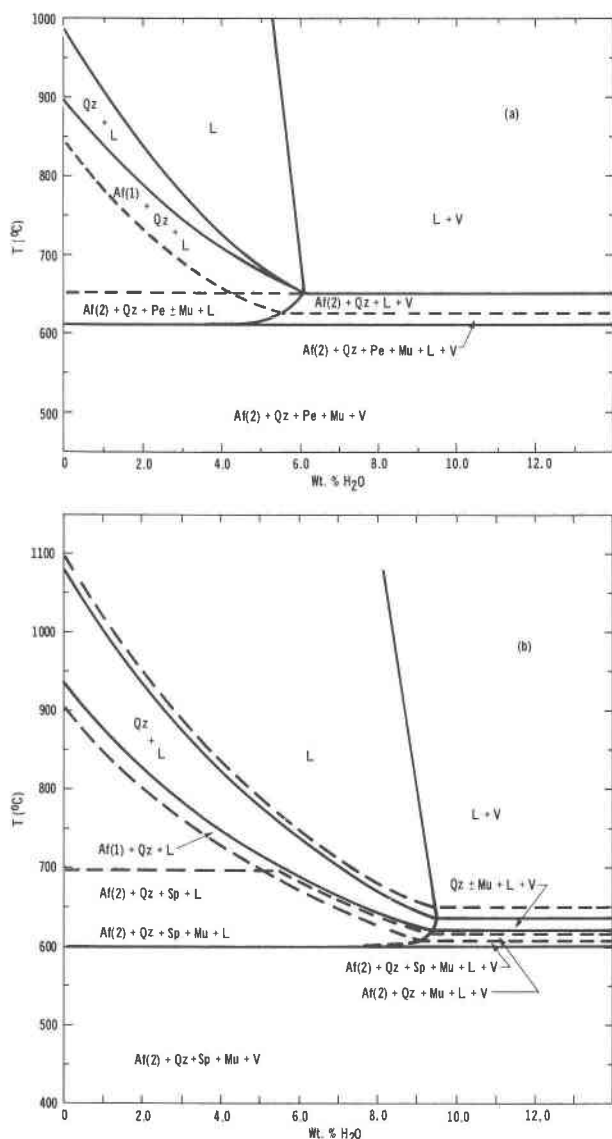
Fig. 10. Phase-assemblage diagrams for the Harding pegmatite (JB-3) at (a) 2.0 and (b) 5.0 kbar, calculated using Equations 3–6 and those in Tables 1 and 2, as well as the PATH program of Nekvasil-Coraor and Burnham (1984). Af(2) = two alkali feldspars, L = liquid (melt), Mu = muscovite mica, Pe = petalite, Qz = quartz, Sp = spodumene, and V = "vapor" (aqueous phase). The stability fields of petalite and spodumene are constrained by the experimentally determined H₂O-saturated solidus (Vaughan, 1963). The stability field of the second (Or-rich) alkali feldspar is calculated from the solvus relations of Thompson and Hovis (1979). Also, the upper, dashed quartz liquidus boundary in Figure 10b is calculated to agree with the experimental results of Burnham and Jahns (1962), as in the text.

clase of An_{68} composition at 840°C, followed by an alkali feldspar of Or_{70} composition at 695°C. Over this wide temperature interval of 145°C, 13 vol% plagioclase crystallizes, and its equilibrium composition changes to An_{29}. Plagioclase (14%, An_{24}) and alkali feldspar (4%, Or_{66}) are

next joined by quartz after a further decrease in temperature of only 5°C (680°C). Owing to the near-minimum composition of the residual melt at the first appearance of quartz, moreover, any further drop in temperature would also cause the residual melt to reach saturation in sillimanite (andalusite?).[13]

Throughout the crystallization interval of 173–185°C, the crystallization of anhydrous phases requires that an H₂O-rich fluid be exsolved by the process of second (resurgent) boiling from an initially H₂O-saturated melt. On the assumption that all of this exsolved H₂O ($X_w^m = 0.479$, 5.97 wt%) is retained in the pegmatite body, the volumetric relations (Burnham, 1972, 1979a, 1979b, 1983, 1985) indicate that the entire body would expand approximately 8.4% upon complete crystallization. In other words, had the Spruce Pine magma undergone closed-system crystallization at a confining pressure of 2.0 kbar (~8 km), the body should contain approximately 8 vol% void space and no primary muscovite. Neither of these features is consistent with the observational evidence.

Had this magma, now saturated with 9.61 wt% H₂O, undergone closed-system crystallization at 5.0 kbar, on the other hand, the pegmatite would contain less than 2.5 vol% void space. As shown in Figure 9b, the sequence of crystallization begins at 5.0 kbar, as before, with plagioclase (An_{75}) at 780°C. At approximately 695°C, according to the experimental results of Vaughan (1963), muscovite would join plagioclase, and the two would crystallize together as temperatures decrease to 660–650°C, where they would be joined by quartz. Within 2 to 10°C, depending upon the muscovite content (cf. Reaction 18), an alkali feldspar of Or_{80} composition would appear ($T \sim 650$°C) after 13–14 vol% of the magma had crystallized and plagioclase had attained an equilibrium composition of An_{33}. The remaining 86–87% of the melt, therefore, must have crystallized over an interval of only 10–15°C, before becoming completely solid at 640°C (Fig. 9b).

The fact that quartz and alkali feldspar, which constitute approximately 80% of the bulk composition of the entire body crystallize virtually simultaneously and over a temperature interval of only 10 or 15°C, has important petrogenetic implications. First and foremost, it accounts for the development of graphic intergrowths of quartz and Or-rich feldspars (perthite) as cotectic precipitates from the melt that are characteristic of the outer intermediate zones (Zones 3 and 4 of Cameron et al., 1949; Norton, 1983) of granitic pegmatites the world over (Jahns, 1955, 1982; Jahns and Burnham, 1969). The fact that the intergrowths of quartz do not commonly extend to the inner terminations of the individual giant perthite crystals, many of which are tapered (Jahns and Burnham, 1969, Fig. 5B;

---

[13] According to the data of Chatterjee and Johannes (1974), which are also represented in Figure 8, the muscovite stability field lies approximately 50°C below the JB-5 solidus at 2.0 kbar. Also, from the work of Holdaway (1971), it appears that the sillimanite-andalusite boundary may intersect the JB-5 solidus at approximately 2.0 kbar.

Table 3. Chemical analyses, norms, and component mole fractions of the Spruce Pine (JB-5) and Harding (JB-3) pegmatites

Constituent	wt. %	CIPW Norm		X_i^{am} (8-oxygen mole)		Constituent	wt.%	CIPW Norm		X_i^{am} (8-oxygen mole)	
SiO_2	73.79	Qz	28.98	$\overline{qz}$	0.314	SiO_2	75.24	Qz	34.00	$\overline{qz}$	0.363
TiO_2	0.050	Co	1.250	$\overline{co}$	0.012	TiO_2	0.05	Co	1.80	$\overline{co}$	0.017
Al_2O_3	15.11	Or	23.94	$\overline{or}$	0.224	Al_2O_3	14.42	Or	17.13*	$\overline{or}$	0.158*
Fe_2O_3	0.260	Ab	40.17	$\overline{ab}$	0.399	Fe_2O_3	0.14	Ab	36.37	$\overline{ab}$	0.356
FeO	0.160	An	4.810	$\overline{an}$	0.045	FeO	0.35	An	0.54	$\overline{an}$	0.005
MnO	0.050	Hy	0.360	$\overline{hy}$	0.0025	MnO	0.18	Hy	0.83	$\overline{hy}$	0.006
MgO	0.070	Mt	0.360	$\overline{mt}$	0.002	MgO	0.01	Mt	0.18	$\overline{mt}$	0.001
CaO	0.970	Il	0.150	$\overline{Il}$	0.0005	CaO	0.20	Il	0.16	$\overline{Il}$	0.001
Na_2O	4.71					Na_2O	4.23	Ap	0.12	$\overline{ap}$	0.001
K_2O	4.02					K_2O	2.74	Be	0.65	$\overline{be}$	0.007
Li_2O	0.010					Li_2O	0.65	Sp	8.22	$\overline{sp}$	0.085
P_2O_5	0.010					P_2O_5	0.13				
						Rb_2O	0.19				
						Cs_2O	0.05				
						BeO	0.09				
						F	0.64				

*The mole numbers of Rb_2O and Cs_2O were combined with that of K_2O in Or and $\underline{or}$.

also see the logo of this issue), also has possible implications for the transition from dominantly melt to dominantly aqueous-phase control of textures. Furthermore, the fact that roughly 80% of the mass of magma crystallizes over the narrow interval of 10–15°C and releases heat only to the extent of approximately 38 cal·g⁻¹ of melt crystallized has implications for the thermal regime of giant crystal growth.

The relatively large temperature interval over which plagioclase and muscovite crystallize from JB-5 melts at 5.0 kbar (Fig. 9b) is consistent with the association of plagioclase and muscovite in the Spruce Pine pegmatite, as well as in most sheet mica–producing pegmatites (Cameron et al., 1949; Norton, 1983). This consistent association notwithstanding, however, the fact that most of this muscovite occurs in the marginal parts of pegmatites (Zones 1 and 2 of Cameron et al., 1949) has led to the common assumption that it forms in response to the selective transport of alkalis, chiefly Na, out of the magma and into the wall rocks (cf. Norton, 1983, p. 872). Although this process doubtless operates in the marginal parts of hydrous magma bodies, it can be effective in the selective leaching of alkalis only if the aqueous fluids are rich in HCl, in which case they would be plagioclase destructive and the equilibrium assemblage would be muscovite + quartz + K-feldspar (Burnham, 1967, 1979b), instead of muscovite + quartz + plagioclase. In other words, the concentration of both muscovite and plagioclase in the typical Zone 1 and 2 assemblages (Cameron et al., 1949) is not consistent with an origin primarily by selective loss of alkalis from this zone through aqueous phase transport.

Another line of evidence that is permissive of an origin of muscovite-rich zones in the Spruce Pine and other pegmatite by internal redistribution of constituents, within an essentially closed magmatic system, is the total muscovite content of the pegmatite relative to its "solubility" in granitic melts. Thus, recasting the normative corundum content of JB-5 (1.25 wt%, Table 3) into its muscovite

equivalent yields 4.8 wt% muscovite, whereas recasting the solubility of sillimanite in granitic melts at 760°C (3.5–4.0 wt%; Voigt, 1983; Joyce, 1985) into its muscovite equivalent yields 8.3–9.5 wt%. The Spruce Pine magma, therefore, was initially undersaturated with respect to sillimanite (at liquidus temperatures, but apparently became saturated with this mineral at approximately 685°C.

It is noteworthy that the bulk muscovite content of several homogeneous Li-rich pegmatites listed by Stewart (1978, Table 1) ranges from 5 to 8 wt% and that the median muscovite content of pegmatitic Harney Peak granite, South Dakota, is 8 wt% (J. J. Norton, cited in Stewart, 1978, p. 975). This cutoff essentially at the equivalent of sillimanite saturation at approximately 750°C suggests that magmatic and hydrothermal processes, operating essentially within *closed* systems, largely control the occurrence and distribution of muscovite in these rocks, including the zoned Spruce Pine pegmatite. The problem, then, is to understand the internal processes by which muscovite and other minerals are concentrated into specific assemblages that occupy certain structural positions (zones) in many pegmatite bodies (cf. Norton, 1983). Unfortunately, the "happy day" when this problem is fully resolved has not yet arrived, but progress has been made and additional constraints will be imposed in subsequent paragraphs.

Harding pegmatite. The phase relations for JB-3 composition in Figures 10a and 10b possess several remarkable features. One of these features is the low temperatures of the H_2O-saturated liquidus and solidus as compared with those of JB-5 composition, especially at low pressures. These temperatures are so low, in fact, that *two* alkali feldspars, quartz, and muscovite could be stable above the solidus at 2.0 kbar (Figs. 8, 10a, 10b). As shown in Figure 10a, quartz and alkali feldspar of Or_{15} composition are calculated to appear on the H_2O-saturated liquidus at 660°C, which is within 5°C of the experimental results of Burnham and Jahns (1962) presented in Figure 8. In these calculations, which utilized Equations 3–6 and

those in Tables 1 and 2, it was assumed that all normative spodumene and corundum in Table 3 reacted to produce 0.142 mol of *pe* (Eq. 17) and 0.062 mol of *dpy,* respectively, and to consume a total of 0.102 mol of *qz* (Si_4O_8). Had it not been assumed that these reactions proceeded essentially to completion, a_{qz}^{am} (X_{qz}^{am}) would have been higher and the calculated quartz liquidus temperature would have been correspondingly higher by 7°C per mole percent Si_4O_8 (*qz*). It was also assumed that the 0.64 wt% of F (0.96 mol% H_8F_8) reacted with 3.84% *ab* to produce 0.96% *cr,* 1.72% *dpy,* and 1.6% *qz,* in accordance with Reaction 19. In view of the excellent agreement between the calculated and experimental temperature, earlier findings regarding the nature and extent of these speciation reactions appear to be confirmed, as is the collective power of the thermodynamic and speciation models to accurately predict phase relations in such compositionally complex systems.

The next phase calculated to appear in H_2O-saturated JB-3 melt at 2.0 kbar is an alkali feldspar of ~Or_{50} composition at a temperature only a few degrees below the appearance of the albitic feldspar and quartz. Hereafter, the sequence of crystallization cannot be calculated precisely, owing to uncertainties regarding the thermal stability of muscovitic mica in the presence of an F- and Li-rich melt (cf. Munoz, 1971; Munoz and Ludington, 1977). The fact that a muscovitic mica appears on the H_2O-saturated JB-3 liquidus only at high pressures (Burnham and Jahns, 1962) and at temperatures 50°C or more below its appearance in JB-5 composition melts (Fig. 8), despite the greater normative corundum content of JB-3 (Table 3), suggests that lithian muscovite is either a near-solidus or subsolidus phase at 2.0 kbar. On this basis, then, petalite is assumed to be the next phase to crystallize from JB-3 composition at 625°C, after two-thirds of the melt has crystallized ($F_m = 0.338$).[14]

The phase-assemblage diagram at 5.0 kbar in Figure 10b differs from that at 2.0 kbar in that muscovite presumably crystallizes early in hydrous JB-3 melts and spodumene, instead of petalite, is the last major phase to appear above the H_2O-saturated solidus. Also unlike the system at 2.0 kbar, the same assumptions regarding speciation to form *pe, dpy,* and *cr* result in a calculated quartz liquidus temperature of 635°C, which is 15°C lower than the experimental temperature in Figure 8. To bring the calculated and experimental temperatures into agreement requires an increase in a_{qz}^{am} (X_{qz}^{am}) of 0.02, which can be readily accomplished by assuming that not all of the *sp* reacts with *qz* to produce *pe* in accordance with Reaction 17. Thus, if 0.03 mol of *sp,* out of a total of 0.085 mol (Table 3), remain as *sp* component in the melt at 5.0 kbar, then the melt contains 0.05 fewer moles of *pe* and 0.02 more moles of *qz* than originally assumed. Moreover, if this shift in the position of equilibrium in Reaction 17

remains linear with pressure, none of the *sp* component would react with *qz* to produce *pe* at pressures greater than 10 kbar. The slope of the JB-3L curve is fully consistent with this linear shift in the *sp-pe* equilibrium, as is the slope of the JB-3S curve. Were it not for this shift, the JB-3S curve should have a slope similar to that of the JB-5S curve in Figure 8.

If the small amount of muscovite that may crystallize as the second phase at 5.0 kbar is neglected for the moment, quartz will be joined by an albitic feldspar of Or_{10} composition at 620°C. This albite will be joined, in turn, by another alkali feldspar of Or_{60} composition at approximately 615°C. At 605–610°C and approximately 66% crystallinity, spodumene will join this subsolvus, two-feldspar plus quartz assemblage, and the last melt will disappear at 600°C. If, on the other hand, muscovitic mica appears before the Or-rich alkali feldspar, as it almost certainly does in this system at 5.0 kbar, then the Or-rich feldspar will not appear until much of the 6.2 mol% muscovite has crystallized at a temperature probably close to that for the first appearance of spodumene (~610°C).

This latter sequence of crystallization, approximately 95% of which occurs over a temperature interval of only 20°C (Fig. 10b), corresponds to the zonal distribution of mineral assemblages in the Harding pegmatite, as described by Jahns and Ewing (1977, p. 119). Thus, the wall zone "is rich in *quartz, albite,* and *muscovite* but is in large part very coarse grained" (italics ours). Beneath this zone "is a continuous layer of massive *quartz,* 2 to 8 feet thick," much of which must have been deposited from the aqueous phase (see below). The massive quartz zone is underlain "by a spectacular *quartz–lath spodumene* zone" that is 2–13 m thick (Jahns, 1953, Fig. 1; Jahns and Ewing, 1977, Fig. 9). This giant spodumene zone is underlain, in turn, by a "core" composed mostly of "spotted rock, . . . a relatively even-grained aggregate of *spodumene, microcline,* and *quartz,* with various combinations of accompanying finer-grained *albite,* lithium-bearing *muscovite,* lepidolite, microlite, and tantalite-columbite."

The remarkable correspondence between the calculated sequence of crystallization and the progressively inward development of mineral zones in both the Harding and Spruce Pine pegmatites strongly suggests that magmatic processes are primarily responsible for the mineral zonation in pegmatites, although this zonation is enhanced and extensively modified by both hypersolidus and subsolidus autometasomatic processes. The occurence of large masses of beryl in the wall zone of the Harding pegmatite, instead of in the "spotted rock core," for example, is indicative of large-scale aqueous-phase transport, as is the "continuous layer" of massive quartz between the wall zone and the quartz–lath spodumene zone. Certain aspects of this aqueous-phase transport will be examined in the next—and last—section; first, however, the significance of the occurrence of quartz on the liquidus of JB-3 composition at pressures within the stability field of primary spodumene, as well as of plagioclase on the liquidus of JB-5 composition, should be briefly examined.

---

[14] The initial *pe* content of JB-3 is 14.2 mol%, and the *pe* content of the melt in Figure 3b at petalite saturation is 42.0 mol%; hence, $F_m = 14.2/42 = 0.338$ at the first appearance of petalite, and the estimated temperature at which this fraction of anhydrous melt equivalent remains is 625°C.

To the extent that JB-3 accurately represents the bulk composition of the original Harding pegmatite magma—and it is probably one of the most representative samples of pegmatite ever collected—the occurrence of quartz on the liquidus at pressures within the stability field of spodumene, whether saturated with H_2O or not (Figs. 8 and 10b), implies that only quartz, or the assemblage quartz + muscovite, was in equilibrium with melt of JB-3 composition at its source. If the Harding magma was completely molten at its source, therefore, this source could not have been a differentiating granitic magma. If, however, as little as 4% residual quartz was present, then the magma would also have been in equilibrium with an albitic alkali feldspar and could, as a consequence, have been derived through differentiation of a very H_2O- and Na-rich, but Ca-poor, parent magma. The Spruce Pine pegmatite magma also could readily have been derived by differentiation of a plagioclase-bearing, but Mg-, Fe-, and P-depleted, parent magma. Both magmas, on the other hand, could equally well have been derived by anatexis of muscovite-bearing, but biotite-poor metamorphic rocks of vastly different origins.

AQUEOUS FLUIDS AND MINERAL ZONING

Figure 5B of Jahns and Burnham (1969), which has been reproduced as the logo at the front of this memorial issue, illustrates several features of pegmatites that are so common as to require explanation by any realistic genetic model. Foremost among these features is the mineral zonation that was interpreted by Jahns and Burnham (1969, p. 856–859) as predominantly a primary feature produced in the presence of both an aqueous phase and an H_2O-saturated melt. The finding above that the inward succession of zones characterized by the abundance of a particular igneous mineral or mineral assemblage corresponds to the sequence of crystallization from the melt phase upon cooling supports this interpretation, as do the results described by Jahns (1982, p. 302), Stewart (1978), and Jolliff et al. (1986). It does not, however, shed much light upon the actual process or processes by which these minerals commonly become segregated into large masses of rock that are almost monomineralic in some cases (quartz cores). Nor does it shed light upon the cause for the vertical asymmetry of units (zones) depicted in the "logo pegmatite" as it will be referred to hereinafter.

This asymmetry, which is expressed as an upward enrichment in K-rich feldspar (perthite "hoods") and a quantitatively complementary downward enrichment in Na-rich feldspar (Jahns, 1982, p. 298), was ascribed by Jahns and Tuttle (1963) to the buoyant ascent of K-rich aqueous-fluid bubbles, leaving behind an Na-enriched magma from which an albitic feldspar precipitates. Subsequent experimental work, with and without chloride solutions (Burnham, and Anderson and Burnham in Clark, 1966; Burnham, 1967; Kilinc, 1969) clearly indicates, however, that the K number [100 K/(K + Na)] in the magmatic aqueous phase is never greater than in the coexisting melt, unless the melt is also in equilibrium with

a K-poor, Na-rich mineral such as hornblende (cf. Burnham, 1979b, p. 116–123) or tourmaline. These experimental results indicate, in fact, that the K numbers of fluids in equilibrium with melts only, whether chloride-bearing or not, are essentially the same as the K numbers of the melts, as expected from the thermodynamic model presented previously. When a mica—either muscovite or biotite—also is present, on the other hand, the K number decreases by as much as 20, thereby providing a possible explanation for the vertical asymmetry that still retains the essential elements of the mechanism proposed by Jahns and Tuttle (1963).

Thus, as the H_2O-saturated "logo pegmatite" magma loses heat through the footwall, as well as the hanging wall, crystallization and concomitant exsolution of an aqueous phase by second (resurgent) boiling results in the formation of aqueous-fluid bubbles which, upon reaching some critical size, will begin to rise from the footwall zone into overlying hotter magma. Upon rising out of the stability field of mica, the fluid bubbles exchange Na for K in the surrounding melt until the K number in the fluid reaches that in the melt. As a result of this exchange and the relatively small size of the ascending bubbles, numerous centers of crystallization of albitic feldspar develop, giving rise to the relatively fine grained texture of the products (cf. Jahns, 1955, Fig. 20). The aqueous fluid bubbles, meanwhile, continue to ascend through the inner, hotter portions of the body and eventually accumulate under the downward-crystallizing carapace, where the lower-temperature phase assemblage again buffers the K number at lower values. The resultant reverse of the previous exchange reaction, therefore, leads to precipitation of K-rich feldspar in the presence of much larger volumes of aqueous fluid, hence fewer centers of crystallization, than in the lower parts of the body.

The efficacy of this process, the later stages of which may be likened to potassic alteration in porphyry copper systems (cf. Burnham, 1979b), depends upon the alkali transport capacity of the magmatic aqueous phase. This transport capacity, in turn, depends upon the Cl content of these fluids, because Cl-poor fluids have very low total normative feldspar contents at all but very high pressures and high temperatures (Fig. 5). A Cl content equivalent to 4–5 wt% NaCl, which appears to be typical of pegmatite fluids (Weisbrod and Poty, 1975; Taylor et al., 1979), should be effective in producing the asymmetry at hypersolidus and immediately subsolidus temperatures, regardless of pressure. They should be especially effective, moreover, in the downward transport of Na and upward transport of K once closed-system convective circulation of these fluids is established. At the same time, however, chloride solutions are singularly ineffective in transporting Al (Burnham, 1967, Fig. 2.7), which is required if the nearly monomineralic bodies of quartz that occur in the "core" zone of the "logo pegmatite" are to be produced.

The bodies of massive quartz in the "core" of the "logo pegmatite" are associated with masses of "pocket pegmatite" that contain abundant crystal-lined cavities (Jahns,

1982, p. 305). These cavities, which are abundant only in shallow-seated pegmatites, such as those in southern California (Taylor et al., 1979), presumably are primary features that represent the segregation and accumulation of aqueous fluids as crystallization of pegmatite magma proceeds both upward and downward from the footwall and hanging wall, respectively. By association, then, much of the massive quartz is presumed to have crystallized from magma; the remainder (~60%) is presumably of subsolidus hydrothermal origin, although the actual mechanism of transport and deposition remains to be determined.

CLOSING STATEMENT

In closing this tribute to an outstanding geologist, who was perhaps as much at home in vertebrate paleontology as in pegmatite petrology, attention is directed again to the opening quotation. Thanks in large measure to the manifold efforts and insights of Dick Jahns, "that happy day which the formation of pegmatite minerals is much more thoroughly understood in terms of P-T-X conditions" is now much closer at hand.

ACKNOWLEDGMENTS

REFERENCES

Anderson, G.M., and Burnham, C. Wayne. (1965) The solubility of quartz in supercritical water. American Journal of Science, 263, 494–511.
——— (1967) Reaction of quartz and corundum with aqueous chloride and hydroxide solutions at high temperatures and pressures. American Journal of Science, 265, 12–27.
——— (1983) Feldspar solubility and the transport of aluminum under metamorphic conditions. American Journal of Science, 283-A, 283–297.
Arndt, J., and Haberle, F. (1973) Thermal expansion and glass transition temperatures of synthetic glasses of plagioclase-like compositions. Contributions to Mineralogy and Petrology, 39, 175–183.
Bell, P.M., and Roseboom, E.H., Jr. (1969) Melting relationships of jadeite and albite to 45 kilobars with comments on melting diagrams of binary systems at high pressures. In J.J. Papike, Ed., Pyroxenes and amphiboles: Crystal chemistry and phase petrology. Mineralogical Society of America Special Paper Number 2, 151–161.
Blencoe, J.G., Merkel, G.A., and Seil, M.K. (1982) Thermodynamics of crystal-fluid equilibria, with applications to the system $NaAlSi_3O_8$-$CaAl_2Si_2O_8$-SiO_2-$NaCl$-$CaCl_2$-H_2O. In S.K. Saxena, Ed., Advances in physical geochemistry, 191–222. Springer-Verlag, New York.
Birch, Francis. (1966) Compressibility; elastic constants. In S.P. Clark, Ed., Handbook of physical constants, 167–173. Geological Society of America Memoir 96.
Boettcher, A.L. (1970) The system CaO-Al_2O_3-SiO_2-H_2O at high pressures and temperatures. Journal of Petrology, 11, Part 2, 337–379.
Boettcher, A.L., and Burnham, C. Wayne. (1983) The structure of silicate liquids: A note. Journal of Geology, 91, 607–608.
Boettcher, A.L., and Wyllie, P.J. (1969) Phase relationships in the system $NaAlSiO_4$-SiO_2-H_2O to 35 kilobars pressure. American Journal of Science, 267, 875–909.
Boettcher, A.L., Burnham, C. Wayne, Windom, K.E., and Bohlen, S.R. (1982) Liquids, glasses and the melting of silicates to high pressures. Journal of Geology, 90, 127–138.
Boettcher, A.L., Guo, Qiti, Bohlen, S.R., and Hanson, Brooks. (1984) Melting in feldspar-bearing systems to high pressures and the structures of aluminosilicate liquids. Geology, 12, 202–204.
Bohlen, S.R., Boettcher, A.L., and Wall, V.J. (1982) The system albite-H_2O-CO_2: A model for melting and activities of water at high pressures. American Mineralogist, 67, 451–462.
Bohlen, S.R., Boettcher, A.L., Wall, V.J., and Clemens, J.D. (1983) Stability of phlogopite-quartz and sanidine-quartz: A model for melting in the lower crust. Contributions to Mineralogy and Petrology, 83, 270–277.
Bowen, N.L. (1913) The melting phenomena of the plagioclase feldspars. American Journal of Science, Fourth Series, 35, No. 210.
Burnham, C. Wayne. (1967) Hydrothermal fluids at the magmatic stage. In H.L. Barnes, Ed., Geochemistry of hydrothermal ore deposits, 1st edition, 34–76. Holt, Rinehart and Winston, New York.
——— (1972) The energy of explosive volcanic eruptions. Earth and Mineral Sciences, Pennsylvania State University, 41, No. 9, 69–70.
——— (1975a) Water and magmas: A mixing model. Geochimica et Cosmochimica Acta, 39, 1077–1084.
——— (1975b) Thermodynamics of melting in experimental silicate-volatile systems. Fortschritte der Mineralogie, Special Issue, IMA-Papers, Ninth Meeting Berlin-Regensburg, 101–118.
——— (1979a) The importance of volatile constituents. In H.S. Yoder, Ed., The evolution of the igneous rocks, fiftieth anniversary perspectives, 439–482. Princeton University Press, New Jersey.
——— (1979b) Magmas and hydrothermal fluids. In H.L. Barnes, Ed., Geochemistry of hydrothermal ore deposits, 71–136. John Wiley and Sons, New York.
——— (1981) The nature of multicomponent aluminosilicate melts. In D.T. Rickard and F.E. Wickman, Eds., Chemistry and geochemistry of solutions at high temperatures and pressures, physics and chemistry of the earth, 13 and 14, 197–229. Pergammon Press, New York.
——— (1983) Deep submarine pyroclastic eruptions. In H. Ohmoto and B.J. Skinner, Eds., The Kuroko and related volcanogenic massive sulfide deposits, 142–148. Economic Geology Monograph 5.
——— (1985) Energy release in subvolcanic environments: Implications for breccia formation. Economic Geology, 80, 1515–1522.
Burnham, C. Wayne, and Davis, N.F. (1974) The role of H_2O in silicate melts: II. Thermodynamic and phase relations in the system $NaAlSi_3O_8$-H_2O to 10 kbar, 700° to 1100°C. American Journal of Science, 274, 902–940.
Burnham, C. Wayne, and Jahns, R.H. (1962) A method for determining the solubility of water in silicate melts. American Journal of Science, 260, 721–745.
Burnham, C. Wayne, Darken, L.S., and Lasaga, A.C. (1978) Water and magmas: Application of the Gibbs-Duhem equation: A response. Geochimica et Cosmochimica Acta, 42, 277–280.

Cameron, E.N., Jahns, R.H., McNair, A.H., and Page, L.R. (1949) Internal structure of granitic pegmatites. Economic Geology Monograph 2.

Chatterjee, N.D., and Johannes, Wilhelm (1974) Thermal stability and standard thermodynamic properties of synthetic $2M_1$-muscovite, $KAl_2[AlSi_3O_{10}(OH)_2]$. Contributions to Mineralogy and Petrology, 48, 89–114.

Clark, S.P., Ed. (1966) Handbook of physical constants. Geological Society of American Memoir 97.

Davis, N.F. (1972) Experimental studies in the system sodium-alumina trisilicate-water: Part 1: The apparent solubility of albite in supercritical water. Ph.D. thesis, Pennsylvania State University, University Park.

Denbigh, Kenneth. (1971) The principles of chemical equilibrium. Cambridge University Press, Cambridge, England.

Dingwell, D.B., Harris, D.M., and Scarfe, C.M. (1984) The solubility of H_2O in the system SiO_2-Al_2O_3-Na_2O-K_2O at 1 to 2 kbar. Journal of Geology, 92, 387–395.

Erikson, R.L. (1979) An experimental and theoretical investigation of plagioclase melting relations. M.S. thesis, Pennsylvania State University, University Park.

Ghiorso, M.S., Carmichael, I.S.E., and Moret, L.K. (1979) Inverted high-temperature quartz. Unit cell parameters and properties of the α-β inversion. Contributions to Mineralogy and Petrology, 68, 307–323.

Ghiorso, M.S., Carmichael, I.S.E., Rivers, M.L., and Sack, R.O (1983) The Gibbs free energy of mixing of natural silicate liquids; an expanded regular solution approximation for the calculation of magmatic intensive variables. Contributions to Mineralogy and Petrology, 39, 175–183.

Gibbs, J.W. (1961) The scientific papers of J. Williard Gibbs, Vol. 1: Thermodynamics. Dover Publications, New York.

Goldsmith, J.R. (1980) The melting and breakdown reactions of anorthite at high pressures and temperatures. American Mineralogist, 65, 272–284.

Goranson, R.W. (1938) Silicate-water systems: Phase equilibria in the $NaAlSi_3O_8$-H_2O and $KAlSi_3O_8$-H_2O systems at high temperatures and pressures. American Journal of Science, 35-A, 71–91.

Hards, N.J. (1976) Distribution of elements between the fluid phase and silicate melt phase of granites and nepheline syenites. NERC Report of Progress in Experimental Petrology, 3, 88–90.

Hariya, Y., and Kennedy, G.C. (1968) Equilibrium study of anorthite under high pressures and temperatures. American Journal of Science, 278, 930–942.

Hervig, R.L., and Navrotsky, Alexandra. (1984) Thermochemical study of glasses in the system $NaAlSi_3O_8$-$KAlSi_3O_8$-Si_4O_8 and the join $Na_{1.6}Al_{1.6}Si_{2.4}O_8$-$K_{1.6}Al_{1.6}Si_{2.4}O_8$. Geochimica et Cosmochimca Acta, 48, 513–522.

Holdaway, M.J. (1971) Stability of andalusite and the aluminosilicate phase diagram. American Journal of Science, 271, 97–131.

Holloway, J.R. (1971) Internally heated pressure vessels. In G.C. Ulmer, Ed., Research techniques for high pressure and high temperature, 217–258. Springer-Verlag, New York.

Jackson, Ian. (1976) Melting of the silica isotypes SiO_2, BeF_2 and GeO_2 at elevated pressures. Physics of the Earth and Planetary Interiors, 13, 218–231.

Jahns, R.H. (1953) The genesis of pegmatites. I. Occurrence and origin of giant crystals. American Mineralogist, 38, 563–598.

——— (1955) The study of pegmatites. Economic Geology, Fiftieth Anniversary Volume, 104–128.

——— (1982) Internal evolution of pegmatite bodies. In Černý, P., Ed., Granitic pegmatites in science and industry, 293–327. Mineralogical Association of Canada, Short Course Handbook 8.

Jahns, R.H., and Burnham, C. Wayne. (1957) Preliminary results from experimental melting and crystallization of Harding New Mexico pegmatite. (abs.) Geological Society of America Bulletin, 68, 1751–1752.

——— (1969) Experimental studies of pegmatite genesis: I. A

model for the derivation and crystallization of granitic pegmatites. Economic Geology, 64, 843–864.

Jahns, R.H., and Ewing, R.C. (1977) The Harding mine, Taos County, New Mexico. Mineralogical Record, March–April 1977.

Jahns, R.H., and Tuttle, O.F. (1963) Layered pegmatite-aplite intrusives. Mineralogical Society of America Special Paper 1, 78–92.

Jolliff, B.L., Papike, J.J., and Shearer, C.K. (1986) Tourmaline as a recorder of pegmatite evolution: Bob Ingersoll pegmatite, Black Hills, South Dakota. American Mineraologist, 71, 472–500.

Joyce, David. (1985) A phase equilibrium study in the system $NaAlSi_3O_8$-SiO_2-Al_2SiO_5-H_2O at 2 kilobars, and petrogenetic implications. M.S. thesis, Pennsylvania State University, University Park.

Kennedy, G.C., Wasserburg, G.J., Heard, H.C., and Newton, R.C. (1962) The upper three-phase region in the system SiO_2-H_2O. American Journal of Science, 260, 501–521.

Kilinc, I.A. (1969) Experimental metamorphism and anatexis of shales and graywackes. Ph.D. thesis, Pennsylvania State University, University Park.

Kilinc, I.A., and Burnham, C. Wayne. (1972) Partitioning of chloride between a silicate melt and coexisting aqueous phase from 2 to 8 kilobars. Economic Geology, 67, 231–235.

Kushiro, Ikuo. (1980) Viscosity, density and structure of silicate melts at high pressures, and their petrological applications. In R.B. Hargraves, Ed., Physics of magmatic processes, 93–120. Pirnceton University Press, New Jersey.

Lambert, I.B., Robertson, J.K., and Wyllie, P.J. (1969) Melting relations in the system $KAlSi_3O_8$-SiO_2-H_2O to 18.5 kilobars. American Journal of Science, 267, 609–626.

Lasaga, A.C., and Burnham, C. Wayne. (1979) Water and magmas: Another reply. Geochimica et Cosmochimica Acta, 43, 643–647.

Lindsley, D.H. (1966) Melting relations of $KAlSi_3O_8$: Effect of pressure up to 40 kilobars. American Mineralogist, 51, 1793–1799.

London, David. (1983) The magmatic-hydrothermal transition in rare-metal pegmatites: Fluid inclusion evidence from the Tanco mine, Manitoba. (abs.) EOS (Transactions of the American Geophysical Union), 64, 865.

——— (1984) Experimental phase equilibria in the system $LiAlSiO_4$-SiO_2-H_2O: A petrogenetic grid for lithium-rich pegmatites. American Mineralogist, 69, 995–1004.

——— (1986) The magmatic-hydrothermal transition in the Tanco rare-element pegmatite: Evidence from fluid inclusions and phase-equilibrium experiments. American Mineralogist, 71, 376–395.

Luth, W.C. (1969) The systems $NaAlSi_3O_8$-SiO_2 and $KAlSi_3O_8$-SiO_2 to 20 kilobars and the relationship between H_2O content, P_{H_2O} and P_{total} in granitic magmas. American Journal of Science, Schairer Volume, 267-A, 325–341.

Luth, W.C., and Tuttle, O.F. (1969) The hydrous vapor phase in equilibrium with granite and granite magmas. In L.H. Larsen, Ed., Igneous and metamorphic geology. Geological Society of America Memoir 115, 513–548.

Luth, W.C., Jahns, R.H., and Tuttle, O.F. (1964) The granite system at pressures of 4 to 10 kilobars. Journal of Geophysical Research, 69, 759–773.

Manning, D.A.C. (1981) The effect of flourine on liquidus phase relationships in the system Qz-Ab-Or with excess water at 1 kbar. Contributions to Mineralogy and Petrology, 76, 206–215.

Manning, D.A.C., and Pichavant, Michel (1983) The role of fluorine and boron in the generation of granitic melts. In M.P. Atherton and C.D. Gribble, Eds., Migmatites, melting and metamorphism. Proceedings of the Geochemical Group of the Mineralogical Society. Shiva Geological Series. Cheshire, U.K.

Muncill, G. (1984) Chemical diffusion in plagioclase melts and petrological implications. (abs.) Geological Society of America Abstracts with Programs, 16, 603.

Munoz, J.L. (1971) Hydrothermal stability relations of synthetic lepidolite. American Mineralogist, 56, 2069–2087.

Munoz, J.L., and Ludington, Steve. (1977) Fluorine-hydroxyl exchange in synthetic muscovite and its application to muscovite-biotite assemblages. American Mineralogist, 62, 304–308.

Navrotsky, Alexandra, Capobianco, Christopher, and Stebbins, J.F. (1982) Some thermodynamic and experimental constraints on the melting of albite at one atmosphere and high pressures. Journal of Geology, 90, 679–698.

Nekvasil, Hanna. (1985) A theoretical thermodynamic investigation of the system Ab-Or-An-Qz(-H₂O) with implications for melt speciation. Ph.D. thesis, Pennsylvania State University, University Park.

Nekvasil-Coraor, Hanna, and Burnham, C. Wayne. (1983) Thermodynamic modelling of crystallization paths of felsic silicate melts. (abs.) Geological Society of America Abstracts with Programs, 15, 651.

———— (1984) Thermodynamic modelling of crystallization paths in felsic melts: The haplogranite and haplogranodiorite systems. (abs.) Geological Society of America Abstracts with Programs, 16, 609.

Norton, J.J. (1983) Sequence of mineral assemblages in differentiated granitic pegmatites. Economic Geology, 78, 854–874.

Orlowski, H.J., and Koenig, C.J. (1941) Thermal expansion of silicate fluxes in the crystalline and glassy states. Journal of the American Ceramics Society, 24, 80–84.

Pichavant, Michel. (1981) An experimental study of the effect of boron on a water saturated haplogranite at 1 kbar vapour pressure. Contributions to Mineralogy and Petrology, 76, 430–439.

———— (1984) The effect of boron on liquidus phase relationships in the system Qz-Ab-Or-H₂O at 1 kbar. (abs.) EOS (Transactions of the American Geophysical Union), 65, 298.

Robie, R.A., and Waldbaum, D.R. (1968) Thermodynamic properties of mineral and related substances at 298.15 K (25.0°C) and one atmosphere (1.013 bars) pressure and at higher temperatures. U.S. Geological Survey Bulletin 1259.

Robie, R.A., Hemingway, B.S., and Fischer, J.R. (1978) Thermodynamic properties of minerals and related substances at 298.15 K and 1 bar (10⁵ pascals) pressure and at higher temperatures. U.S. Geological Survey Bulletin 1452.

Scarfe, C.M. (1984) Pressure dependence of the viscosity of silicate melts. (abs.) 27th International Geological Congress, Moscow 5, Sections 10–11, 390.

Schairer, J.F., and Bowen, N.L. (1956) The system Na₂O-Al₂O₃-SiO₂. American Journal of Science, 254, 129–195.

Shaw, H.R. (1963) The four-phase curve sanidine-quartz-liquid-gas between 500 and 4000 bars. American Mineralogist, 48, 883–896.

Skinner, B.J. (1966) Thermal expansion. In S.P. Clark, Ed., Handbook of physical constants, 75–96. Geological Society of America Memoir 97.

Stebbins, J.F., Carmichael, I.S.E., and Weill, D.F. (1980) High temperature heat contents, heat capacities and solution properties of plagioclase composition liquids. (abs.) Geological Society of America Abstracts with Programs, 12, 528.

———— (1983) The high temperature liquid and glass heat contents and heats of fusion of diopside, albite, sanidine and nepheline. American Mineralogist, 68, 717–720.

Stewart, D.B. (1967) Four-phase curve in the system CaAl₂Si₂O₈-SiO₂-H₂O between 1 and 10 kilobars. Schweizerische Petrologische Mitteilungen, 47, 35–39.

———— (1978) Petrogenesis of lithium-rich pegmatites. American Mineralogist, 63, 970–980.

Swanson, S.E. (1977) Relation of nucleation and crystal-growth rate to the development of granitic textures. American Mineralogist, 62, 966–978.

Taylor, B.E., Foord, E.E., and Friedrichsen, H. (1979) Stable isotope and fluid inclusion studies of gem-bearing granitic pegmatite-aplite dikes, San Diego Co., California. Contributions to Mineralogy and Petrology, 68, 187–205.

Thompson, J.B., Jr., and Hovis, G.L. (1979) Entropy of mixing in sanidine. American Mineralogist, 64, 57–65.

Tuttle, O.F., and Bowen, N.L. (1958) Origin of granite in light of experimental studies. Geological Society of America Memoir 74.

Vaughan, D.E.W. (1963) The crystallization ranges of the Spruce Pine and Harding pegmatites. M.S. thesis, Pennsylvania State University, University Park.

Voigt, D.E. (1983) The solubility of Al₂SiO₅ in the system KAlSi₃O₈-SiO₂-H₂O at 2 kbar, and its implications for melt speciation. M.S. thesis, Pennsylvania State University, University Park.

Wardle, R. (1972) A structural study of pyrophyllite, 1Tr and its dehydroxylate. Ph.D. thesis, Pennsylvania State University, University Park.

Waldbaum, D.R. (1968) High-temperature thermodynamic properties of alkali feldspars. Contributions to Mineralogy and Petrology, 17, 71–77.

Weill, D.F., Stebbins, J.F., Hon., R., and Carmichael, I.S.E. (1980) The enthalpy of fusion of anorthite. Contributions to Mineralogy and Petrology, 74, 95–102.

Weisbrod, Allen, and Poty, Bernard. (1975) Thermodynamics and geochemistry of the hydrothermal evolution of the Mayres pegmatite, southeastern Massif Central (France). Petrologie, 1, no. 1-16, 89–102.

Wood, B.J. (1978) Reaction involving anorthite and CaAl₂SiO₆ pyroxenes at high pressures and temperatures. American Journal of Science, 278, 930–942.

Wyllie, P.J., and Tuttle, O.F. (1961) Experimental investigation of silicate systems containing two volatile components: Part II. The effects of NH₃ and HF, in addition to H₂O on the melting temperatures of albite and granite. American Journal of Science, 259, 128–143.

Yoder, H.S. (1954) The system diopside-anorthite-water. Carnegie Institution of Washington Year Book, 53, 106–107.

APPENDIX 1. NOTATION

General thermodynamic notation

a relative activity
C_P isobaric heat capacity
$\bar{G}$ molal Gibbs free energy
$\bar{H}$ molal enthalpy
k Henry's law analogue constant
P pressure
R universal gas constant
T temperature in kelvins (K)
$\bar{V}$ molal volume
X mole fraction; $X(E)$ is the mole fraction at the binary eutectic
α isobaric thermal expansion
β isothermal compressibility
γ activity coefficient

Abbreviations and subscript notations

A unspecified crystalline aluminosilicate (feldspar)
a unspecified aluminosilicate component
Ab   albite (analbite)
ab albite-like component ($NaAlSi_3O_8$)
An   anorthite
an anorthite-like component ($CaAl_2Si_2O_8$)
Ap   apatite
ap dehydroxylated apatite-like species ($Ca_{3.08}P_{1.846}O_8$)

Be   normative beryl
be   beryl-like species ($Be_{1.33}Al_{0.89}Si_{2.67}O_8$)
Co   corundum
co   corundum-like species ($Al_{5.33}O_8$)
cr   cryolite-like species ($Na_4Al_{1.33}F_8$)
Cts   calcium Tschermak's pyroxene
dpy   dehydroxylated pyrophyllite–like species ($Al_{1.455}Si_{2.91}O_8$)
Eu   eucryptite
eu   eucryptite-like species ($Li_2Al_2Si_2O_8$)
gr   grossularite-like species ($Ca_2Al_{1.33}Si_2O_8$)
Hy   normative hypersthene
hy   hypersthene-like species [$(Mg,Fe)_{1.33}Si_{2.67}O_8$]
I   unspecified crystalline phase
i   unspecified nonvolatile component
Il   normative ilmenite
il   ilmenite-like species ($Fe_{2.67}Ti_{2.67}O_8$)
J   unspecified crystalline phase other than I
j   unspecified nonvolatile component with which component *i* interacts
kts   potassium tetrasilicate–like species ($K_{1.78}Si_{3.56}O_8$)
Ky   kyanite
L   liquid (melt) phase
Lc   leucite
lc   leucite-like species ($K_{1.33}Al_{1.33}Si_{2.67}O_8$)
m*i*   referring to the melting of pure phase I
Mt   normative magnetite
mt   magnetite-like species (Fe_6O_8)

nds   sodium disilicate–like species ($Na_{3.2}Si_{3.2}O_8$)
ns   sodium silicate–like species ($Na_{2.53}Si_{3.37}O_8$)
ntb   sodium tetraborate–like species ($Na_{2.286}B_{4.571}O_8$)
Or   sanidine
or   sanidine-like component ($KAlSi_3O_8$)
Pe   petalite
pe   petalite-like species
Qz   quartz
qz   quartz-like component (Si_4O_8)
Sil   sillimanite
sil   sillimanite-like species ($Al_{3.2}Si_{1.6}O_8$)
Sp   spodumene
sp   spodumene-like species ($Li_{1.33}Al_{1.33}Si_{2.67}O_8$)
V H_2O-rich volatile phase ("vapor")
w H_2O
Zo   zoisite
zo   zoisite-like species ($Ca_{1.28}Al_{1.92}Si_{1.92}O_8$)

Superscript notations

am   anhydrous melt
g   in the glassy state
hm   hydrous melt
m   melt with unspecified H_2O content
°   pertaining to the 1-bar and T standard state
s   in the solid state